

ORIGINAL PAPER

Ultrastructure of *Gyrodinium spirale*, the Type Species of *Gyrodinium* (Dinophyceae), Including a Phylogeny of *G. dominans*, *G. rubrum* and *G. spirale* Deduced from Partial LSU rDNA Sequences

Gert Hansen^{a,1} and Niels Daugbjerg^b

^aIOC Science & Communication Centre on Harmful Algae, Biological Institute, Øster Farimagsgade 2D, DK-1353 Copenhagen, Denmark

^bDepartment of Phycology, Biological Institute, University of Copenhagen, Øster Farimagsgade 2D, DK-1353 Copenhagen, Denmark

Submitted September 8, 2003; Accepted March 23, 2004
Monitoring Editor: Donald M. Anderson

A detailed ultrastructural analysis of the type species of *Gyrodinium*, *G. spirale*, was made based on cells collected from Skagerrak and southern Kattegat (Denmark). This material is considered very similar to the type material studied by Bergh from southern Kattegat. The analysis revealed many characters typical for dinoflagellates as well as a number of previously undescribed features. Here, emphasis was given to a three-dimensional configuration of the flagellar apparatus, the surface ridges, and the nuclear capsule. The latter had a rather complex ultrastructure consisting of two wall-like layers surrounded by membranes, with nuclear pores restricted to globular invaginations of these layers. To overcome difficulties with culturing of many auto- and heterotrophic dinoflagellates, we designed a specific reverse primer to amplify ca. 1800 base pairs of nuclear-encoded LSU rDNA. Using this approach, LSU rDNA sequences were determined from three heterotrophic species of *Gyrodinium*, including the type species. Using other alveolates (i.e. ciliates and Apicomplexa) as outgroup species, phylogenetic analyses based on Maximum Likelihood, Maximum Parsimony, and Neighbor-Joining supported *Gyrodinium* as a separate lineage. Unfortunately, the nearest sister group to *Gyrodinium* could not be established due to low bootstraps support for the deep branching pattern.

Introduction

Two major groups of dinoflagellates may be distinguished; (1) thecate species with discernible thecal plates; and (2) athecate or 'naked' species without plates or with plates that are barely visible in the light microscope. At the time when Bergh (1881) did

his investigations near Strib (southern Kattegat, Denmark), only three species of dinoflagellates were considered athecate. These were classified in the genera *Amphidinium* (*A. operculatum* Claparède & Lachmann) and *Gymnodinium* (viz. *G. fuscum*, the type species, and *Gymnodinium pulvisculus* (Ehrenberg) Stein). *Gymnodinium pulvisculus* was later transferred to *Glenodinium* by Stein (1883). Interestingly, Bergh (1881) did not consider *Amphidinium*

¹ Corresponding author;
fax 45 35322321
e-mail gerth@bot.ku.dk

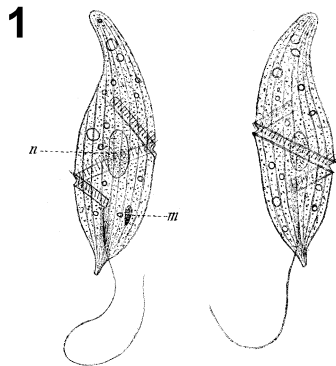


Figure 1. Original illustrations of *Gyrodinium spirale* by Bergh (1881).

and *Gymnodinium* to be related, an idea that has recently received support from nuclear-encoded LSU and SSU rDNA sequence analyses (e.g. Daugbjerg et al. 2000, Flø Jørgensen et al. 2004, Saunders et al. 1997). Bergh (1881) described two new marine *Gymnodinium* species from Strib, *Gymnodinium gracile* Bergh and *G. spirale* Bergh. The latter differed from other *Gymnodinium* species by its characteristic shape and the spiral path of the transverse furrow or cingulum (Fig. 1). Longitudinal surface striations were described for both *G. gracile* and *G. spirale*. Schütt (1896) subsequently created the genus *Spirodinium* with *S. spirale* (Bergh) Schütt as the type species. The main diagnostic characters were that the cingulum followed a spiral path for somewhat more than one turn and the ends were significantly displaced, surface striations were sometimes present, chloroplasts were yellow or absent, and the stigma was absent or very small without a lens. However, the name *Spirodinium* had previously been used for a ciliate (Fiorentini 1890, cited from Fensome et al. 1993) and was illegitimate according to the International Code of Zoological Nomenclature. Kofoid and Swezy (1921) changed the name to *Gyrodinium* and emended the genus, distinguishing *Gyrodinium* from *Gymnodinium* by a cingular displacement of more than 20% of the body length. However, the name *Spirodinium* was still valid under the International Code of Botanical Nomenclature (ICBN), but at the International Botanical Congress in Berlin, the name *Gyrodinium* was conserved (Greuter et al. 1988).

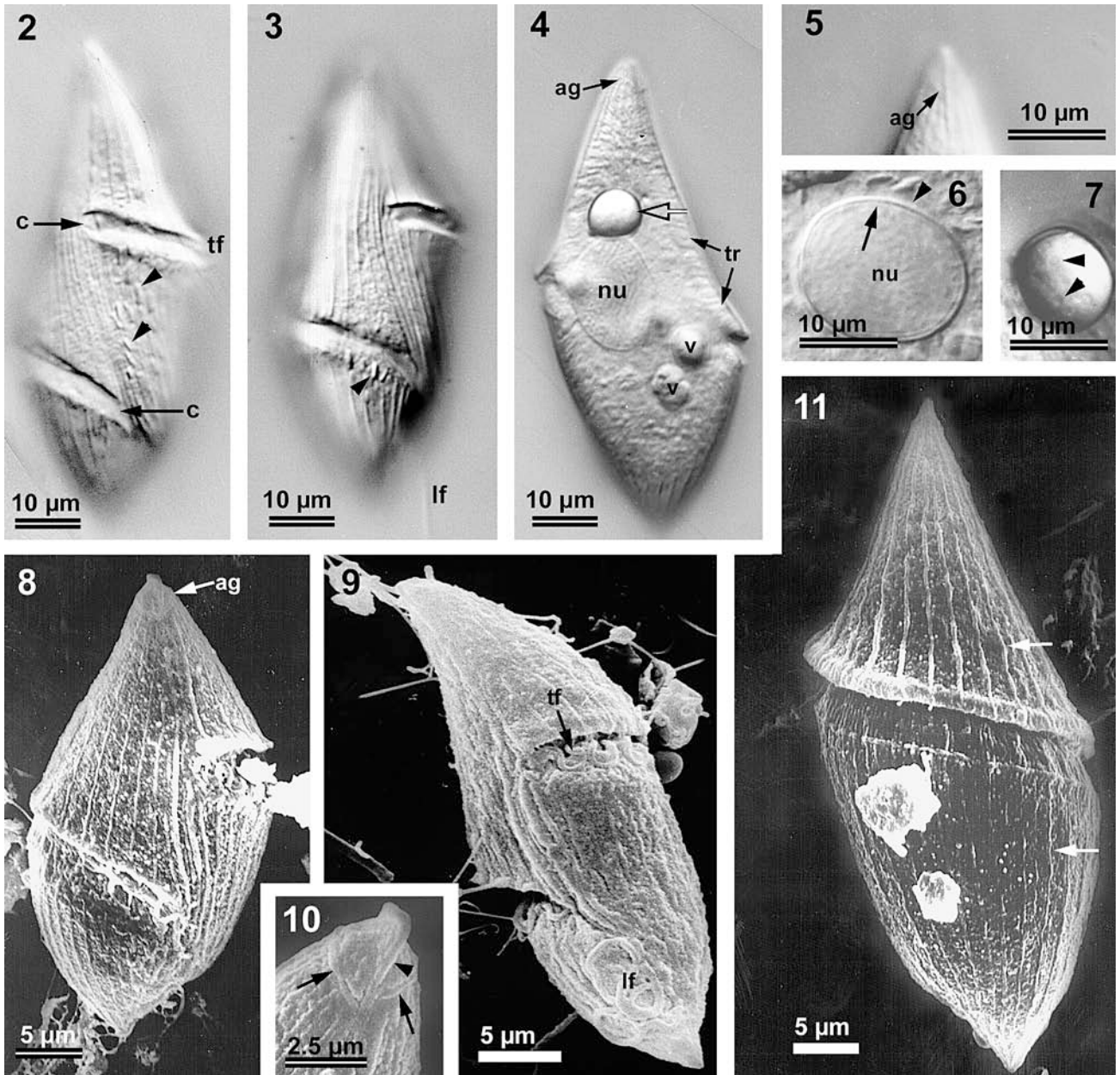
For decades, it has been speculated that a cingular displacement of about 20% is not useful as a separating character at the generic level. Additionally, culture studies have shown that considerable variation of this feature may occur, even within clones (Kimball and Wood 1965). Recently, Daugbjerg et al. (2000) combined ultrastructural features and partial

LSU rDNA sequences to emendate *Gymnodinium* and *Gyrodinium*. According to the new circumscriptions of the genera, the main characteristics of *Gymnodinium* sensu stricto are the presence of a horse-shoe shaped apical groove running in an anti-clockwise direction, a nuclear envelope with vesicular chambers, and a nuclear or dorsal fibrous connective inter-linking the LMR (R1 sensu Moestrup 2000) flagellar root and the nucleus. *Gyrodinium* is heterotrophic and characterised by the presence of surface striations and an elliptical apical groove bisected by a ridge. The aim of this paper is to provide an ultrastructural analysis of *Gyrodinium spirale* as a basis for further emendations of the genus when additional fine-structural data on related species become available. Furthermore, we aimed at elucidating the phylogeny of *Gyrodinium* from nuclear-encoded partial LSU rDNA gene sequences.

Results

Light and Scanning Electron Microscopy

Cells of *Gyrodinium spirale* from Skagerrak show some variation in cell shape, but are most commonly elongated with a somewhat conical epicone, and a pointed or slightly blunted apex, pointing to the right (Fig. 2). The right margin of the epicone is often more or less concave (Figs 2, 9). The hypocone is broader than the epicone and has a small pointed antapical protrusion (Figs 8–9, 11). The cells measure 70–80 μm in length and ca. 30 μm in width. The girdle is displaced ca. 40% of the cell length. A characteristic feature is the longitudinal surface ridges (Figs 2–3, 8–9, 11). The surface ridge lining the right margin of the intercingular region (region between the two cingular ends) continues to the apex (Figs 8–10). An apical groove, barely visible in the light microscope, encircles the apex, and together with the surface ridge, the apex looks like a 'conquistador-like' helmet (Figs 4–5, 10). Numerous trichocysts and/or mucocysts are situated along the cell margin and some cells also have rod-shaped bodies about 2 μm long, perhaps endosymbiotic bacteria (Figs 2–4). The rod-shaped structures were not observed in the sectioned material from Ballen Harbour. A large nucleus is situated centrally in the cell. A distinct nuclear capsule surrounds the nucleus (Figs 4, 6). A distinct spherical refractive body was sometimes present anterior to the nucleus. This structure measured ca. 8 μm in diameter and was surrounded by a wall-like structure with circular surface depressions (Figs 4, 7). Food vacuoles were often present in the posterior part of the cell (Fig. 4).



Figures 2–11. Light and scanning electron microscopy of *Gyrodinium spirale* from Skagerrak. **2–3.** The displaced cingulum (c) with the transverse flagellum (tf) and longitudinal flagellum (lf). Rod-shaped bodies are present along the cell surface (arrowhead). **4.** Deeper focus of a cell revealing the nucleus (nu), food vacuoles (v), and trichocysts (tr) lining the cell periphery. Notice the refractive body (open arrow) and the barely visible apical groove (ag). **5.** Higher magnification of the apical groove. **6–7.** Higher magnification of the nucleus and refractive body in a lysed cell. Notice a thicker (arrowhead) outer and thinner (arrow) inner layer of the nuclear capsule, and also the circular depression of the refractive body (arrowheads in Fig. 7). **8–10.** The apical groove is evident (arrows in Fig. 10). A surface ridge dissects the apical groove and continues to the apex of the cell (arrowhead in Fig. 10). **9** shows both the transverse and the longitudinal flagellum. **11.** Dorsal view of a cell with well preserved surface ridges (arrows).

Transmission Electron Microscopy

Amphiesma: The amphiesma consists of numerous closely abutting vesicles subtending the outer plasma membrane. The vesicles contain electron-dense granular material, but this material is only present in cells fixed as outlined in fixation schedule 2 and may be an artifact (Figs 12–13). Using fixation schedule 1, the amphiesmal vesicles are broken and no trace of dense material is present (Figs 14, 16). Sectioned cells from fixation schedule 1 reveal a very delicate, more or less continuous layer with a somewhat honeycomb-like substructure (Figs 14–16). This layer, obscured by the dense material in cells fixed according to schedule 2, is located between the inner (intact) and outer (broken) amphiesmal membranes (Fig. 14). It seems that two amphiesmal vesicles span the distance between two surface ridges and only one is found across the ridge itself when seen in cross or surface sections (Figs 12, 17), but it is uncertain whether or not this is a consistent feature over the entire cell surface. The amphiesmal vesicles between the surface ridges have a somewhat quadratic appearance in at least part of the cell surface. A layer is situated underneath the amphiesmal vesicles (Fig. 13). This may represent a pellicle *sensu* Höhfeld and Melkonian (1992). Numerous cortical microtubules are situated within and between the surface ridges (Figs 12–14, 16), usually in a single row, but bundles of microtubules within the ridges were occasionally observed (not shown). The surface ridges have an unusual fine structure not yet fully understood. In cross-section, each ridge appears to contain a ‘vesicle’ or chamber constricted by an electron dense ‘plug’; however, when seen in longitudinal sections, these ‘plugs’ run along the entire surface ridge, regularly interrupted by empty-looking regions (Figs 12–14, 16–17). Sometimes, it appears as if two or more ‘vesicles’ and ‘plugs’ are present per ridge, but this may be due to an oblique section angle of the ridge. Longitudinal arrays of mitochondria subtend most of the surface ridges (Figs 12, 18).

The ventral ridge: A ventral surface ridge runs from about the level of the longitudinal flagellar canal and probably up to the level of the exit of the transverse flagellum, although the exact length has not been determined (Figs 13, 44, 50–51). The SEM preparation did not resolve this delicate structure. The ridge consists of two electron dense layers separated by a somewhat fibrillar layer. The central part of the ridge is apparently not to be covered by amphiesma vesicles (Fig. 13). A microtubular band beneath and parallel with the ridge was observed in cells fixed according to fixation schedule 2 (Fig. 13), but it was not apparent in the other fixation. It is un-

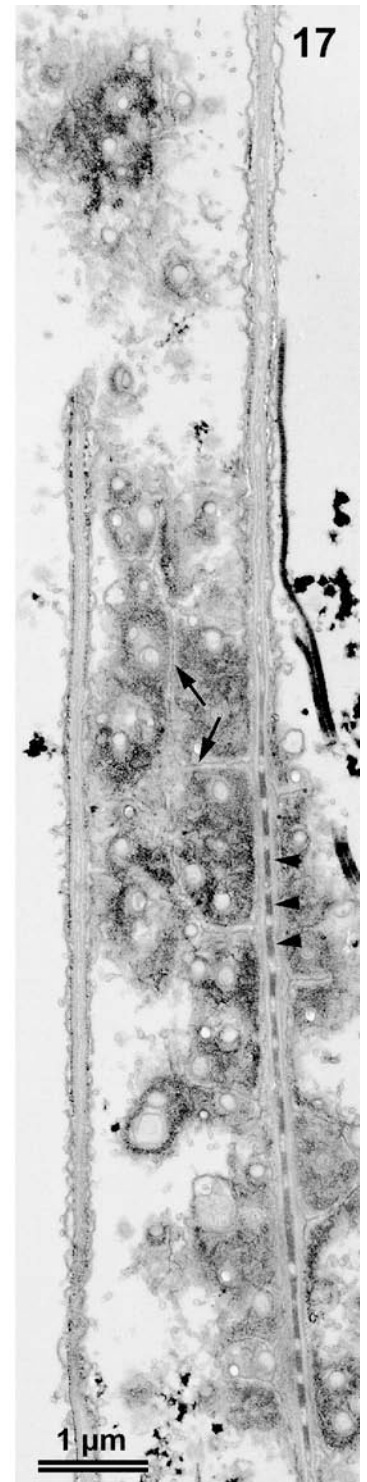
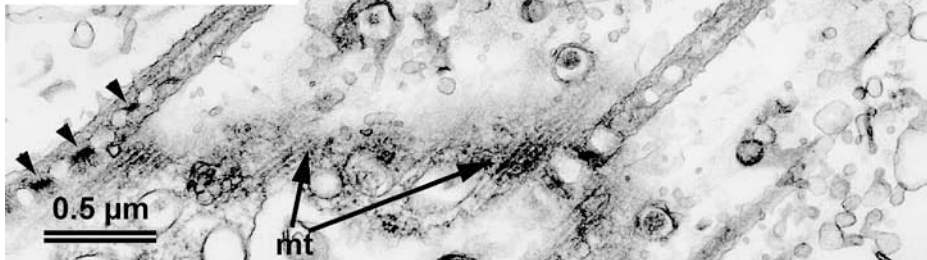
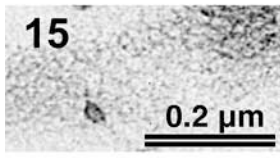
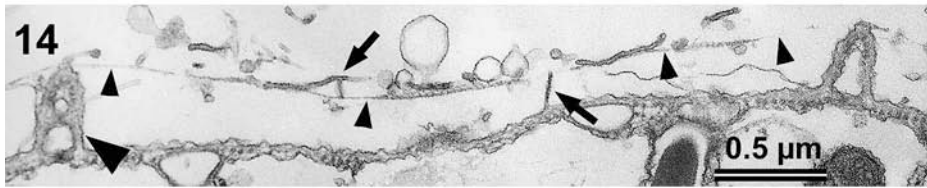
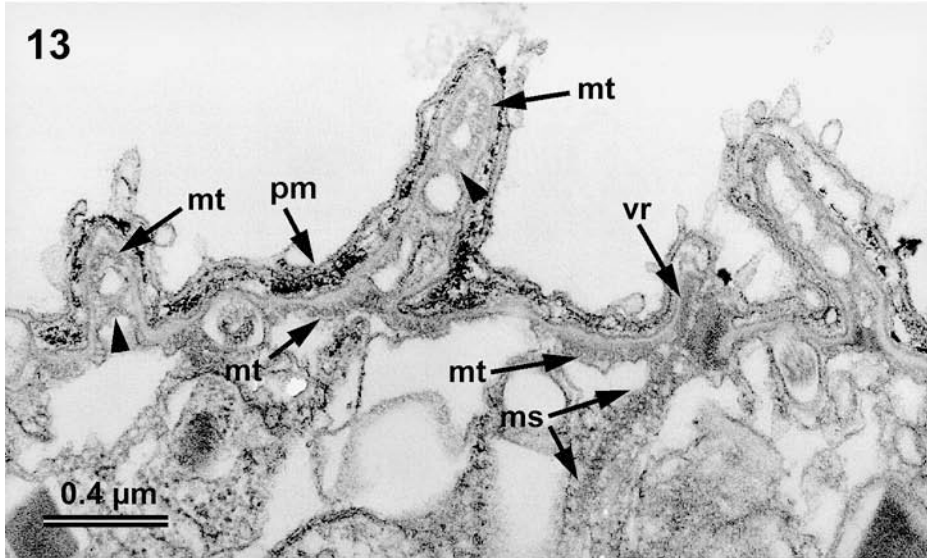
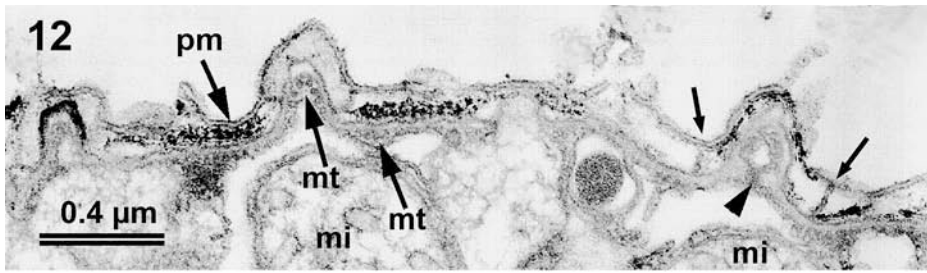
certain whether this microtubular band is present along the entire ventral ridge.

Trichocysts and mucocysts: Numerous trichocysts are present along the periphery of the cell together with vesicles with weakly electron dense contents, interpreted as mucocysts. Together with mitochondria, they appear to be orderly arranged in alternating longitudinal rows (Fig. 18).

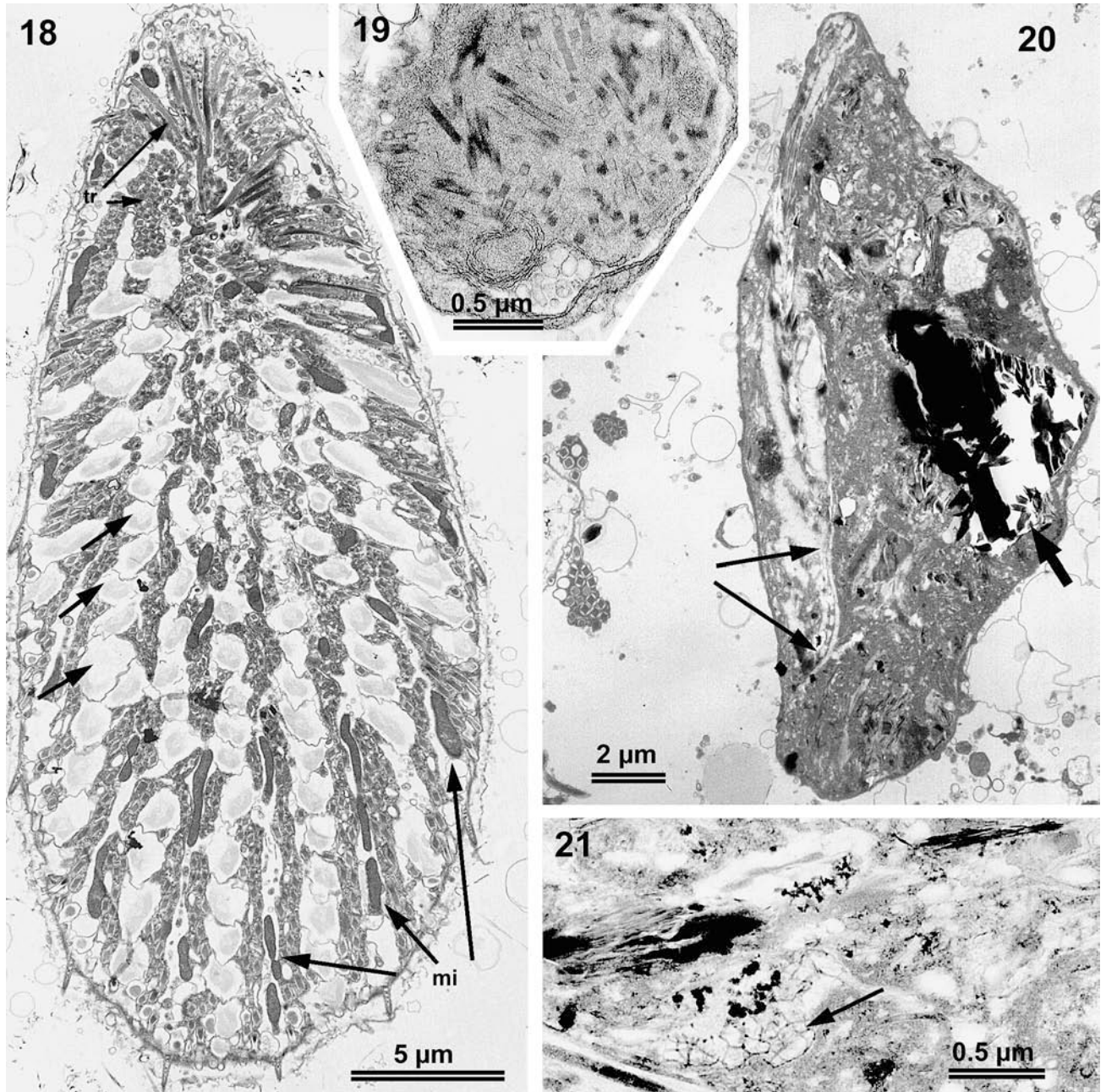
Food vacuoles: A food vacuole with remnants of various prey items was present in one of the sectioned cells. Although the contents appeared to be in a final stage of digestion, traces of bacteria (not shown), *Heterocapsa*-scales, and what appear to be the remnants of diatom frustules could be recognised (Figs 20–21). This indicates that *G. spirale* is quite unselective with respect to prey and prey-sizes. It supports previous laboratory feeding experiments showing a broad prey-size spectrum (Hansen 1992). Accumulation bodies or autophagous vacuoles with numerous trichocyst remnants were also common (Fig. 19). No starch or lipid granules were observed.

The nucleus: Three membranes surround the nucleoplasm, the two innermost representing the nuclear envelope. Two distinct wall-like layers, the outermost being more electron-dense than the other, are located between the nuclear envelope membranes. The gap between the two layers may be an osmotic artifact, but electron-dense material is usually present within this gap in the area around the globular invaginations (Figs 22–30). The inner layer forms ridges into the nucleoplasm and these appear to be arranged in a hexagonal pattern (Fig. 22). Globular invaginations, also formed by the inner layer, are situated along these ridges. At these sites the outer layer also invaginates and together with the inner layer forms a neck-like extension of the globule (Fig. 26). Nuclear pores are 50–55 nm in diameter and restricted to the globular invaginations (Figs 22–29). It is somewhat unclear what happens with the first or outermost membrane at the site of an invagination, but it appears to cover the opening (Figs 25–26, 30). The nucleus of *Gyrodinium spirale* contains normal dinoflagellate chromosomes (Fig. 23). A diagrammatic illustration of what we term the ‘nuclear capsule’ is depicted in Fig. 31.

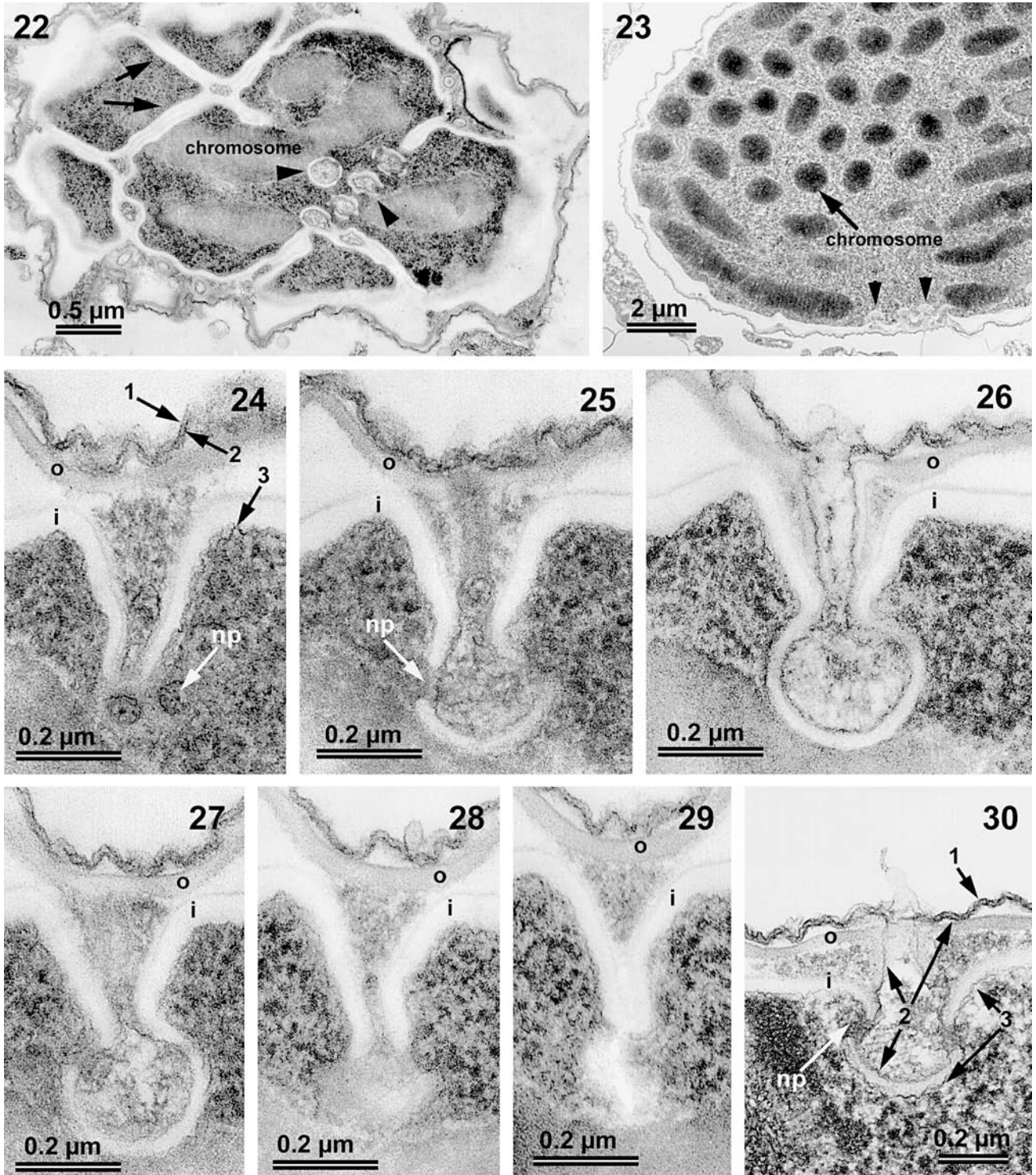
The pusule: One pusule is associated with each of the flagellar canals (Figs 32, 34, 39). The collecting chambers are tubular and continue deep into the cytoplasm (Fig. 34). Numerous pusular vesicles associate with the collecting chamber (Figs 32, 39). It basically conforms to Dodge’s (1972) ‘pusule with collecting chambers branching of the flagellar canal’, although the collecting chamber in *G. spirale* is very long.



Figures 12–17. The amphiesma. **12–13.** Cross-sections of the amphiesma showing dense plug-like structure within a surface ridge (arrowhead). One amphiesmal vesicle covers each ridge (sutures are marked by small arrows). A microtubular strand (ms) is associated with the ventral ridge of the cell (vr). Cortical microtubules (mt) are located within and in-between the surface ridges. pm: plasmalemma; mi: mitochondria. Notice, the granular material inside the amphiesmal vesicles. **14.** Bursting amphiesma vesicles. Arrows point to broken sutures, arrowheads to the continuous layer with a honeycomb-like pattern. **15.** Surface section of the honeycomb-like layer. **16–17.** Tangential surface sections of the amphiesma. The dense material along the surface ridges (arrowheads) and the cortical microtubules between the ridges (mt) are evident. Notice that a row of two square amphiesmal vesicles is located between the surface ridges (arrows). The honeycomb-like layer is marked with arrows in Figure 16.



Figures 18–21. Mucocysts and food vacuole. **18.** Oblique section showing longitudinal arrays of mucocysts (arrows). Mitochondria (mi) and numerous trichocysts (tr) are located between the mucocysts. **19.** Accumulation body containing trichocyst? remains. **20.** Food vacuole probably containing remnants of a diatom frustule (long arrows) and perhaps a small sand grain (thick arrow). **21.** Higher magnification of a food vacuole revealing the presence of *Heterocapsa* scales (arrow).



Figures 22–30. The nucleus. **22.** Surface section of the nucleus partly revealing the hexagonally pattern of the inner layer (arrows). Cross-sections of the globular invaginations are also visible (arrowheads). **23.** Numerous chromosomes. Arrowheads indicate globular invaginations. **24–29.** Adjacent serial sections of the same globular invagination. The outermost membrane is labelled 1, the membranes of the nuclear envelope 2 and 3, respectively. The outer and inner wall layers are labelled o and i, respectively. Notice the nuclear pores (np). **30.** Another globular invagination with a more distinct inner membrane (3).

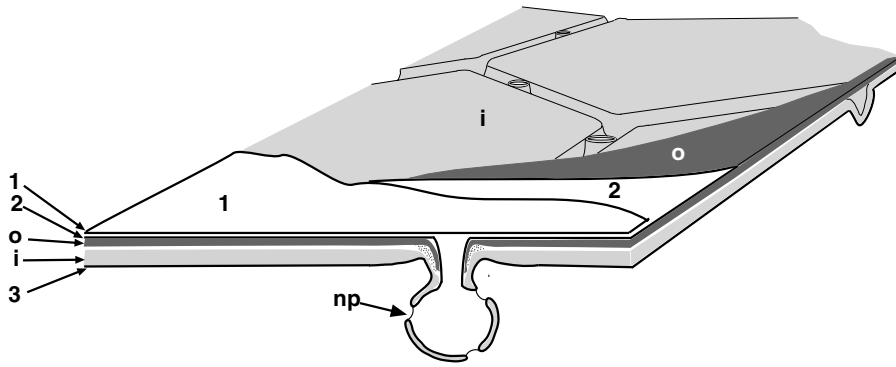


Figure 31. Diagrammatic illustration of the 'nuclear-complex'. Same labelling as in Figure 24.

The flagellar apparatus: The flagellar apparatus is shown in a diagrammatic reconstruction in Fig. 52. It consists of a multimembered microtubular root (LMR or R1) emerging from the longitudinal basal body (LB) (Figs 39–40, 49) and a striated root (TSR) originating from the transverse basal body (TB) (Figs 32–34, 45–48). The TSR proceeds in both an anterior and posterior direction upon its emergence from the proximal part of the TB (Figs 33–36). The LMR and TSR are interconnected by a large striated root connective (src), measuring about 20 μm in length. It has a repeating striation pattern of alternating thick and thin electron dense bands separated by less dense areas (Figs 34–41). Electron-dense fibrous material (f) is associated with the dorsal side of the proximal part of the LMR (Figs 39–41, 49). A single-membered microtubular root (TSRM or R4) appears to emanate from the basal part of the TB continuing along the anterior part of the TSR (Figs 33, 45–46). Another single-membered microtubular root (TMR or R3) also emerges from the basal part of TB (Figs 32, 45–47). It takes an anterior direction along the right side of the flagellar canal (Figs 32, 46) where it nucleates numerous microtubules (TMRE; Fig. 45). Numerous collared pits line the flagellar canal in this area (Figs 32, 45). The basal bodies are oppositely directed and widely separated (ca. 20 μm) (e.g. Figs 47, 49). Tubular structures were sometimes present near the LB (Figs 41–43).

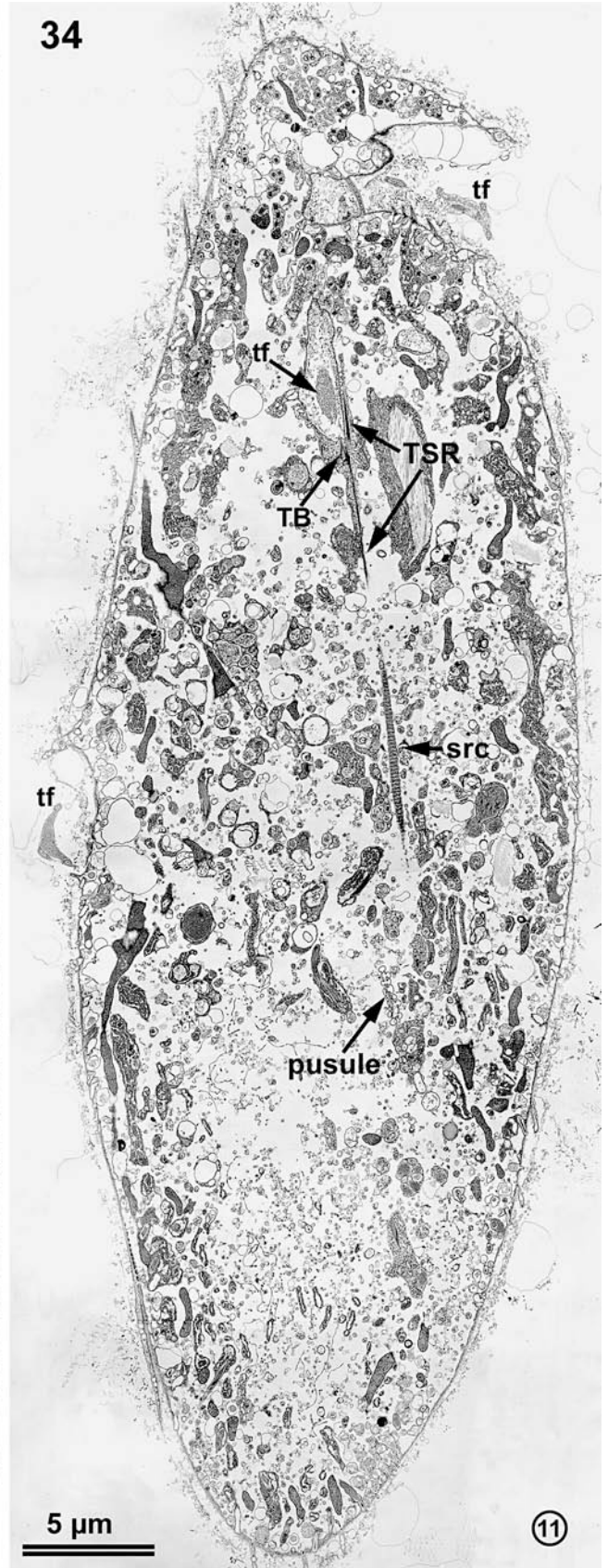
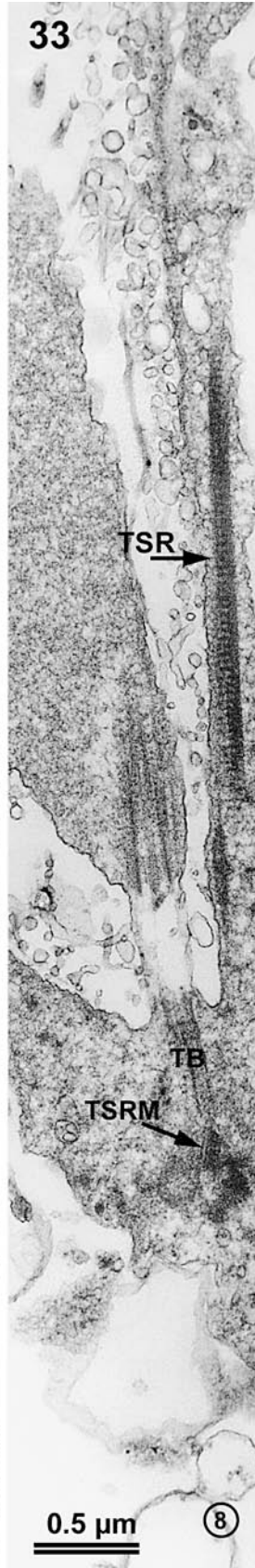
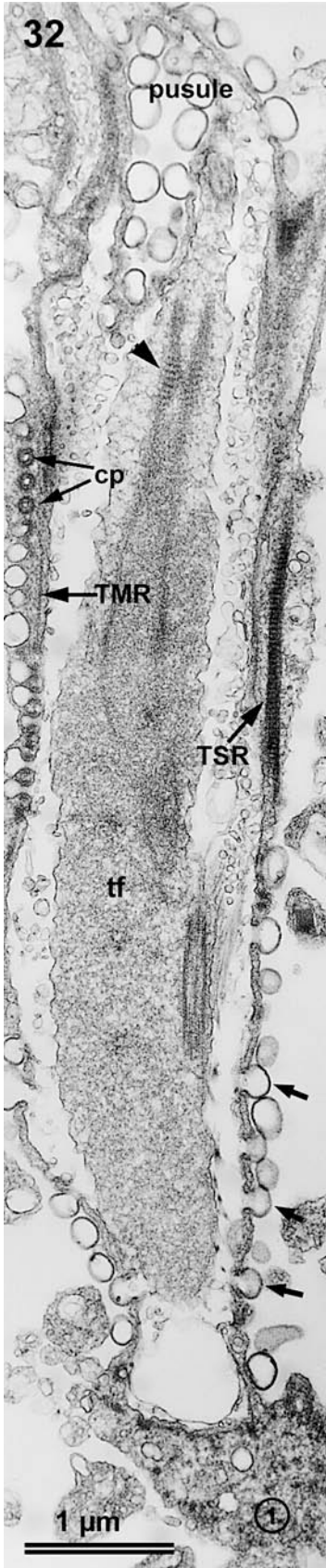
No distinct striated collars are present around the flagellar canals, although electron-dense material partly surrounds the longitudinal flagellar canal (Figs 50–51). This material appears to make contact with the ventral ridge (not shown).

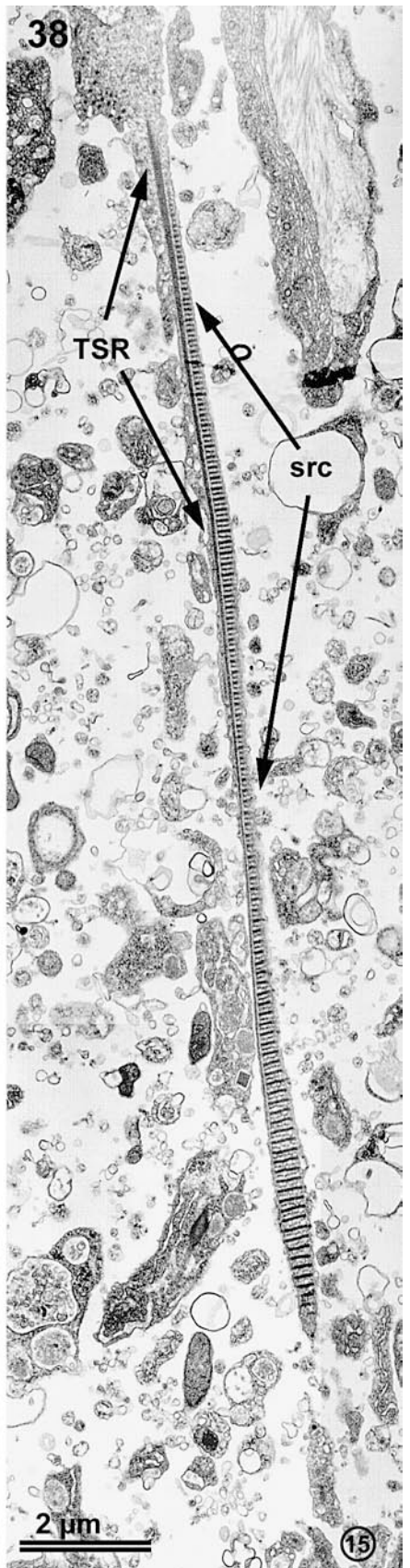
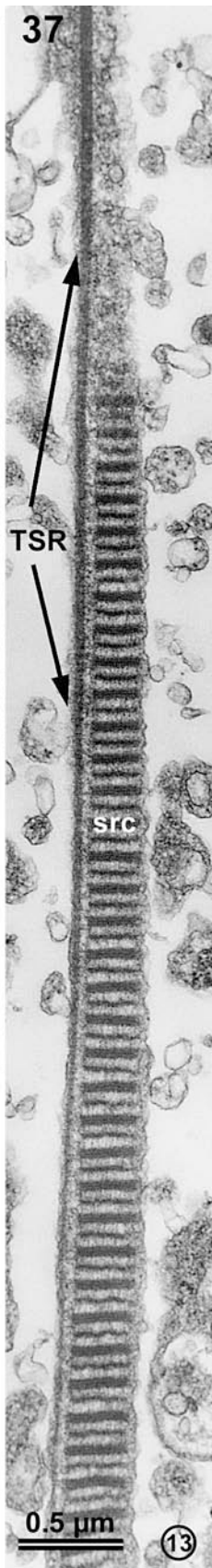
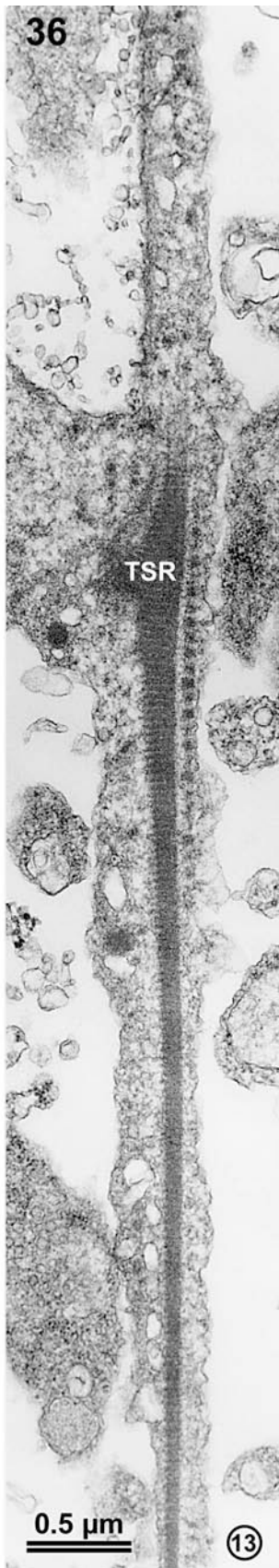
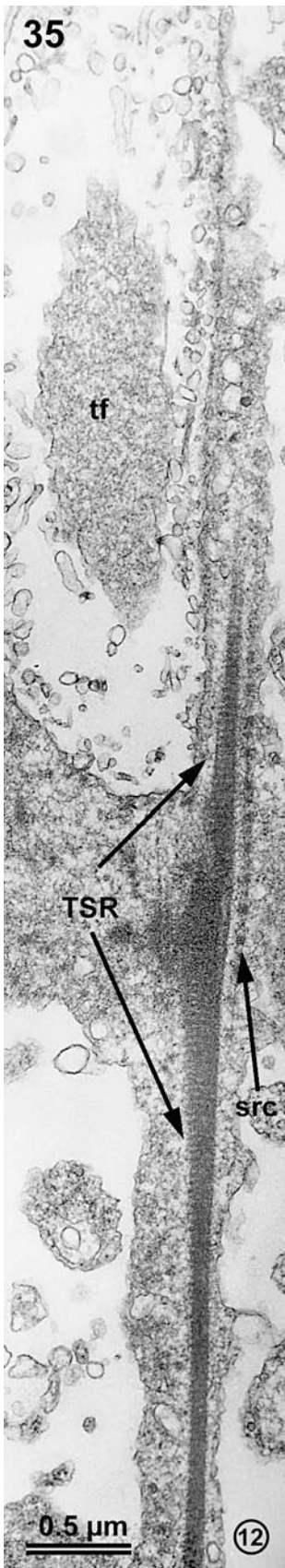
Molecular Data

Specific reverse primer: The design of a reverse primer specific for dinoflagellates among the species of protists available in GenBank as of March 1, 2004, proved to be a successful approach for determination of both DNA strands of the LSU rDNA gene from three species of *Gyrodinium* (viz. *G. spirale*, *G. rubrum*, and *G. dominans*). This primer labelled 'DINO-ND' was also used to successfully amplify approx. 1800 base-pairs of the LSU rDNA gene from *Dinophysis norvegica*, another heterotrophic dinoflagellate determined during this study (see Methods). However, the primer will amplify partial LSU rDNA from organisms of macroscopic origin (e.g. *Rattus norvegicus* [Norway rat], *Mus musculus* [house mouse] and *Homo sapiens* [human], *Drosophila melanogaster* [the fruitfly], and *Oryza sativa* [rice]) if combined with a forward LSU rDNA eukaryotic primer such as D1F. Since these macroscopic organisms would be noticeable in both marine and freshwater samples, we consider the use of the specific reverse primer unproblematic in the way

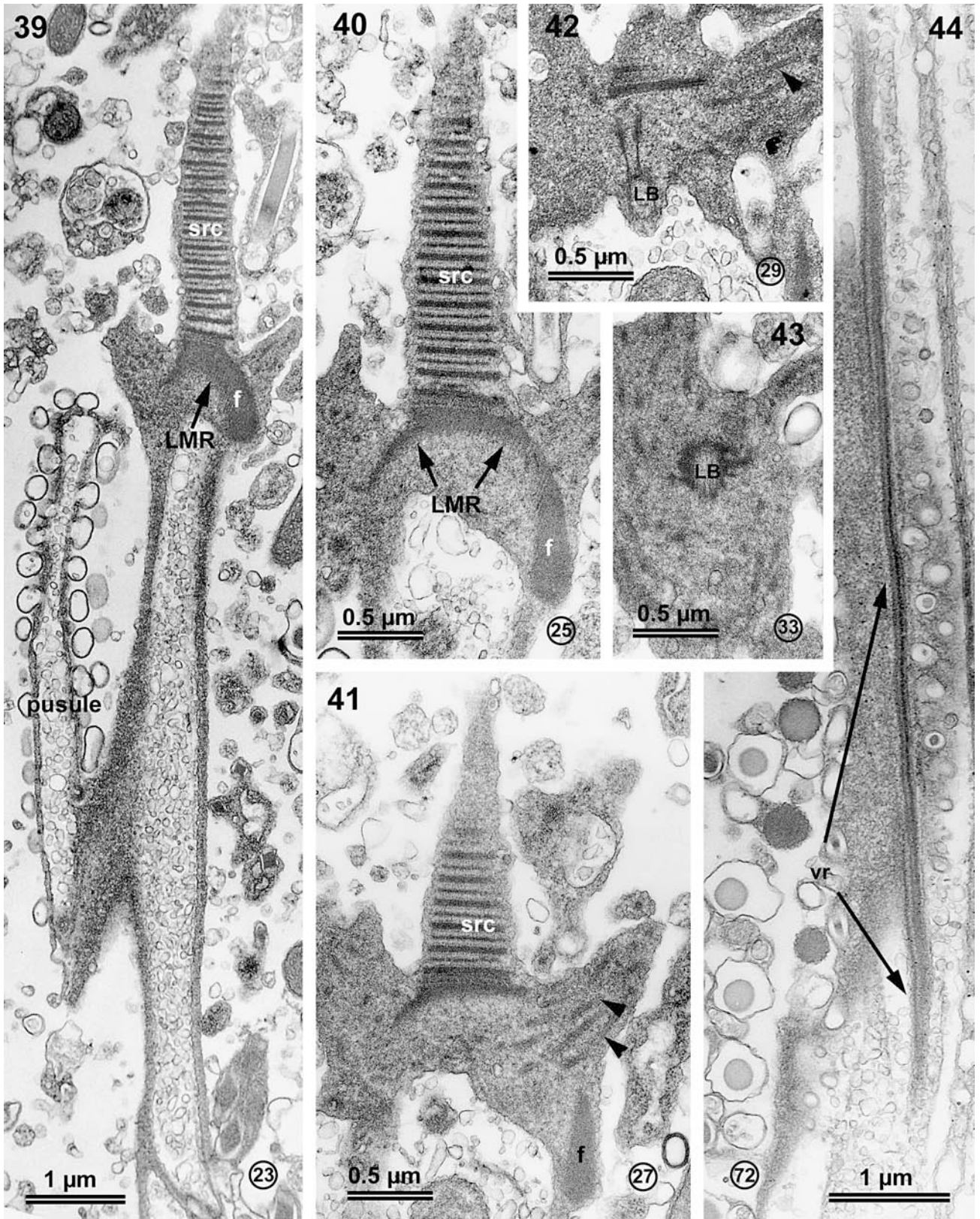
Figures 32–44. Longitudinal sections of the flagellar apparatus and the ventral ridge. Non-adjacent slightly oblique longitudinal serial sections of the flagellar apparatus (small encircled numbers refer to section number). Section sequence is from dorsal/left to ventral/right.

32–33. The TSR and TMR run along the flagellar canal. The proximal part of the TSRM is visible. Pusular vesicles (arrows) and collared pits (cp) are situated along the canal. Notice the striated strand (arrowhead) of the transverse flagellum (tf). **34.** Composite picture of a whole cell. Notice the transverse flagellum (tf) within the cingulum and the pusule to become associated with the longitudinal flagellar canal. The TSR and the src are also visible.

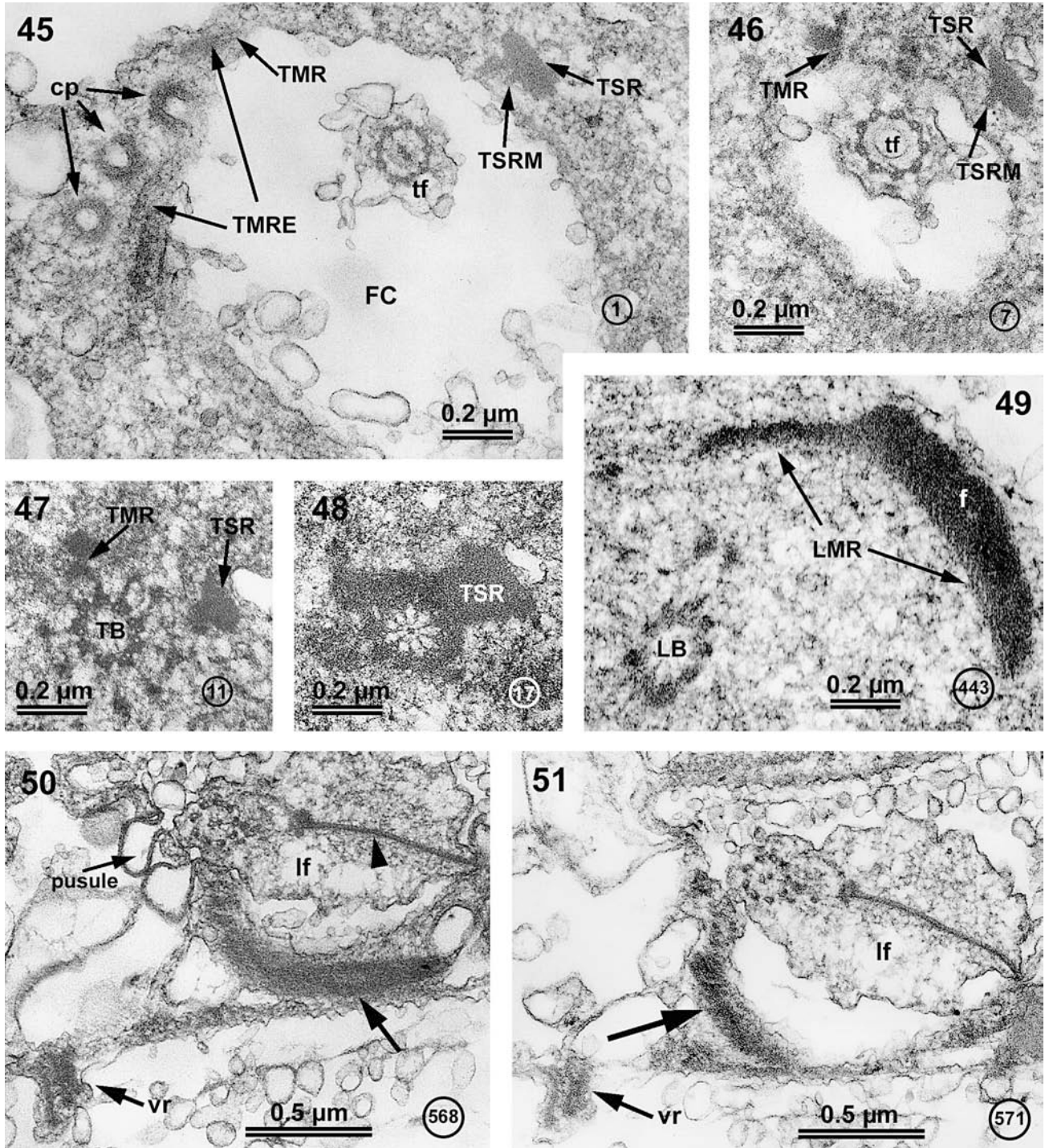




35–38. **35.** The TSR is running in both an anterior and posterior direction. The src is also visible. **36–37.** The same section showing the anterior and posterior portion of the TSR, respectively. Notice also the banding pattern of the src. **38** shows the very thin posterior portion of the TSR and also the src, which continues further posteriorly to connect with the LMR.



39–41. The src connects with the LMR. A fibrous component (f) is associated with the dorsal side of the LMR. Tubular structures are located close to LB (arrowheads). **42–43.** The LB. **44.** Surface section of the ventral ridge (vr).



Figures 45–51. Cross sections of the flagellar apparatus and the ventral ridge. Non-adjacent serial cross sections of the flagellar apparatus (small encircled numbers refer to section number). Section sequence is from anterior to posterior. **45–46** show the transverse flagellar canal. The TMR with associated TMRE and TSR with associated TSRM run along the canal. **47–49.** The transverse basal body (TB). Notice its cartwheel appearance in **48**. **49.** The LB and LMR with associated fibrous component (f). **50–51.** The longitudinal flagellum with paraxonemal rod (arrowhead). Dense fibrous material partly surrounds the flagellar canal (arrow). Notice also the ventral ridge (vr).

applied here. Negative controls containing all PCR reagents except for single cells or extracted DNA were always included to examine for self-contamination.

LSU rDNA of species of *Gyrodinium*: A comparison based on uncorrected p-distances (option in PAUP* 4.0) of 1360 base-pairs (including a few introduced gaps) from the three species of *Gyrodinium* included in this study, revealed a sequence divergence of 6 to 10%. This range is similar to that estimated between species assigned to *Ceratium*, but slightly less than in species of *Alexandrium* Halim, the *Spiniferites-Gonyaulax* group, and *Gymnodinium* (Ellegaard et al. 2003; Hansen et al. 2000a). A few synapomorphies were recorded for the *Gyrodinium* species (not shown).

Phylogeny of *Gyrodinium*: In phylogenetic analyses based on ML, MP, and NJ methods, the three species of *Gyrodinium* formed a monophyletic group supported by high bootstrap support ($\geq 92\%$) (Fig. 53). The sequence data thus, indicates that *Gyrodinium* constitutes a distinct lineage. In ML and MP analyses, *G. rubrum* formed a sister taxon to *G. spirale* and *G. dominans*. However, this topology only received moderate bootstrap support (70% in ML and 57% in MP). On the contrary, *G. dominans* diverged first in NJ analysis (tree not shown). The branching order of the three species of *Gyrodinium* is thus incongruent. Following bootstrap support values obtained in ML, MP, and NJ analyses, the divergence of the deep dinoflagellate lineages could not be recognized with confidence because bootstrap values were below 50% (Fig. 53). Hence, the nearest sister group to the *Gyrodinium* lineage could not be established.

Discussion

Identity of *Gyrodinium spirale*

The cell size and morphological variation in *Gyrodinium spirale* may be quite large. Dodge (1982) quoted a size span of 40–200 μm in length. Feeding experiments performed by Hansen (1992) also demonstrated an extreme variation in morphology during and after food uptake of large prey organisms such as centric diatoms. Schütt (1895) described numerous varieties of *Gyrodinium spirale* (as *Gymnodinium spirale*). Many of these were later raised to species level by Kofoid and Swezy (1921): *Gyrodinium acutum* (Schütt) Kofoid & Swezy, *Gyrodinium cornutum* (Pouchet) Kofoid & Swezy, *Gyrodinium mitra* Kofoid & Swezy, *Gyrodinium obtusum* (Schütt) Kofoid & Swezy, and *Gyrodinium pingue* (Schütt) Ko-

foid & Swezy. Other species with strong resemblance to *Gyrodinium spirale* are *Gyrodinium fusiforme* Kofoid & Swezy, *Gyrodinium lachryma* (Meunier) Kofoid & Swezy, and *Gyrodinium nasutum* (Wulff) Schiller.

Due to the apparent morphological ‘plasticity’ of *G. spirale*, several of these species need to be verified by modern techniques such as SEM, TEM, and nucleotide sequence data.

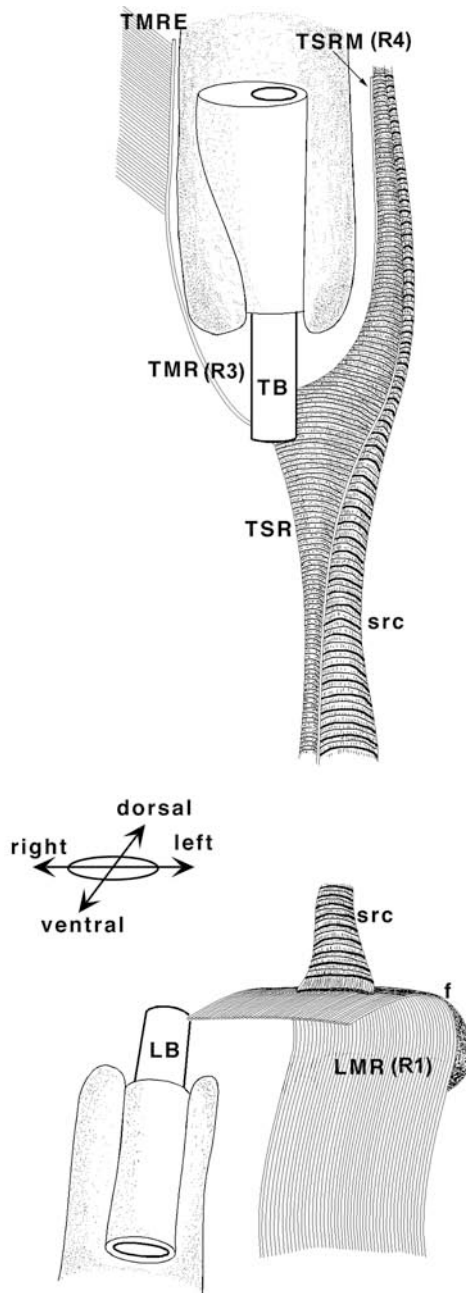


Figure 52. Diagrammatic illustration of the flagellar apparatus.

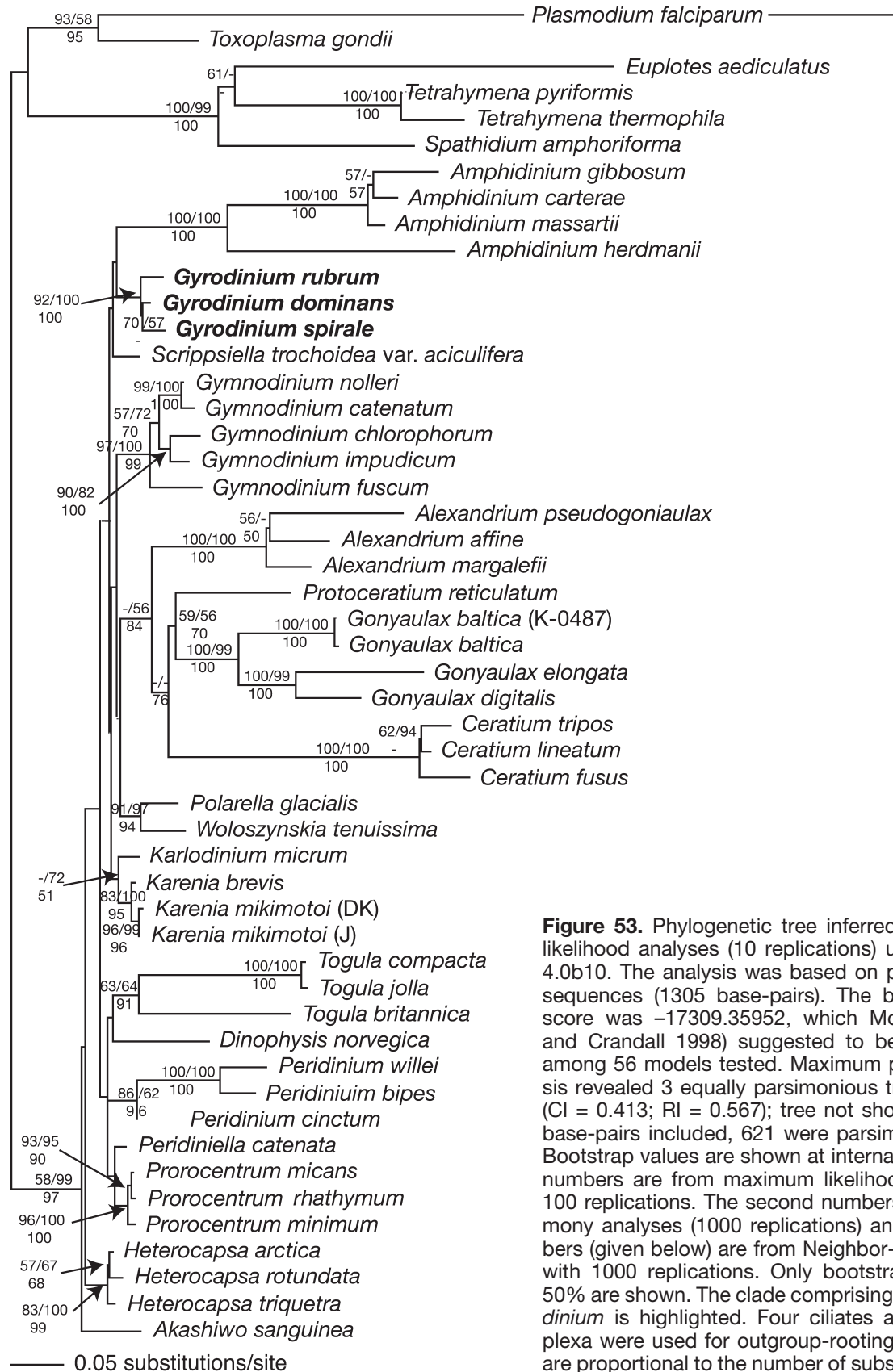


Figure 53. Phylogenetic tree inferred from maximum likelihood analyses (10 replications) using PAUP* ver. 4.0b10. The analysis was based on partial LSU rDNA sequences (1305 base-pairs). The best ln likelihood score was -17309.35952, which Modeltest (Posada and Crandall 1998) suggested to be the best-fitting among 56 models tested. Maximum parsimony analysis revealed 3 equally parsimonious trees, 3714 steps (CI = 0.413; RI = 0.567); tree not shown. Of the 1305 base-pairs included, 621 were parsimony informative. Bootstrap values are shown at internal nodes. The first numbers are from maximum likelihood analyses with 100 replications. The second numbers are from parsimony analyses (1000 replications) and the third numbers (given below) are from Neighbor-Joining analyses with 1000 replications. Only bootstrap values above 50% are shown. The clade comprising species of *Gyrodinium* is highlighted. Four ciliates and two apicomplexa were used for outgroup-rooting. Branch lengths are proportional to the number of substitutions per site.

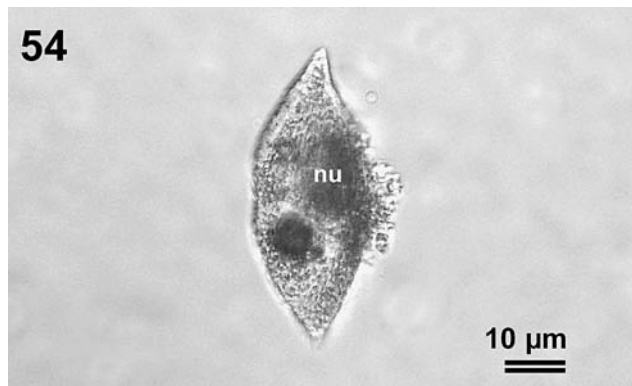


Figure 54. A Lugol-fixed specimen of *G. spirale* from the same water sample and with the same morphotype as the cell used for single-cell PCR analysis. nu: nucleus.

The material used in this study is in good agreement with the original description by Bergh (1881). With respect to size (70–80 μm in the present material, 60–100 μm in the original description) and outer morphology, particularly the bending of the anterior part of the epicone towards the right and the distinct tapering of the antapex (compare Fig. 9 with the original illustration by Bergh shown in Fig. 1). However, it should be noted that these features were not always prominent.

Ultrastructure

The ultrastructure of *Gyrodinium spirale* revealed typical dinoflagellate features, i.e. amphiesma, dinokaryon, trichocysts, mitochondria with tubular cristae, and a flagellar apparatus with typical configuration of the flagellar root system. However, it also contained a number of unusual features, which will be addressed in detail.

The amphiesma: The presence of a layer with a honeycomb-like substructure within the amphiesmal vesicles has also been observed in other unarmored dinoflagellates, e.g. *Amphidinium poecilochroum* Larsen, *Gymnodinium cryophilum* (Wedemayer, Wilcox & Graham) Hansen & Moestrup, *Gymnodinium cf. chlorophorum*, and *Noctiluca scintillans* (Macartney) Kofoid (Honsell et al. 1988; Larsen 1988; Melkonian and Höhfeld 1988; Wilcox et al. 1982). The function of this layer is unknown, but may be related to either the thecal plates or the pellicle (see Höhfeld and Melkonian 1992, Morrill and Loeblich 1983 for detailed discussions). The most intriguing feature of the amphiesma is the electron-dense material within the surface ridges. This has, to our knowledge, not been observed in other

dinoflagellates and is very different than the plug-like structures associated with the inner amphiesmal vesicle membrane of *Karlodinium micrum* (Daugbjerg et al. 2000; Dodge and Crawford 1970; Leadbeater and Dodge 1966). Details of the amphiesma of *G. spirale* were also provided by Brown et al. (1988). Although they did not mention this, the ‘vesicles’ and dense material also seem to be present within the surface ridges in their material (Brown et al. 1988, their Fig. 8). A difference between the material studied here and that used by Brown et al. (1988) is the prominent cortical microtubular bundles present in the latter. We have occasionally observed microtubular bundles within the surface ridges, but not as extensive as in that study. An interesting feature is the arrays of mitochondria subtending most of the surface ridges. Arrays of mitochondria and microtubules seem to play a role in the formation of the raphe canal in raphid diatoms; although once the canal or keels are made, their numbers are reduced considerably (Pickett-Heaps et al. 1990). Perhaps the mitochondria in *G. spirale* have a similar role in providing energy for the formation and maintenance of the surface ridges.

The nuclear capsule: A number of predominantly unarmored dinoflagellates have a wall-like layer surrounding the nucleus (see e.g. Kofoid and Swezy 1921), a feature usually referred to as the nuclear- or perinuclear capsule. Ultrastructural studies of this structure are very limited and in most cases preliminary. The capsules of *Erythroopsis* (spp.?), *Warnovia* (spp.?), *Cochlodinium* (spp.?), and *Protoperidinium depressum* (Bailey) Balech have been studied in some details by Greuet (1972). The capsules according to Greuet consists basically of two main components or layers: a principal or main layer, consisting of an outer annulated and an inner continuous lamella or membrane, and a skeletal layer with a wall- or plate-like and somewhat fibrous appearance. Both layers are located outside the nuclear envelope. The principal layers are apparently lacking in *Protoperidinium depressum* and *Cochlodinium* (spp.?), but the latter has a fibrillar layer adjacent to the nuclear envelope. However, it is not entirely clear whether this fibrillar layer is located inside, outside, or within the nuclear envelope, but from the published micrographs, it appears to be within the nuclear envelope, as it seems to be framed by a pair of unit membranes (Greuet 1972, see Fig. 11a,c). Chamber-like elevations of the inner fibrillar layer occur at regular intervals and the nuclear pores seem to be associated with these chambers (see Fig. 11 in Greuet 1972). The arrangement of the nuclear capsule of *Cochlodinium* (spp.?), *Erythroopsis* (spp.?), *Warnovia* (spp.?), and *Protoperidinium de-*

Table 1. List of dinoflagellates, ciliates, and Apicomplexa (the latter two groups are used as outgroups) included in the phylogenetic study. Strain numbers and GenBank accession numbers (in bold sequences obtained during this study) are also provided (– = data not available).

Taxa	Strain no.	GenBank accession numbers
DINOPHYCEAE		
<i>Akashiwo sanguinea</i> (Hirasaka) Gert Hansen & Moestrup	JL36	AF260396
<i>Alexandrium affine</i> (Inoue & Fukuyo) Balech	–	AY294612
<i>Alexandrium margalefii</i> Balech	–	AY154957
<i>Alexandrium pseudogoniaulax</i> (Biecheler) Horiguchi ex Kita & Fukuyo	–	AY154958
<i>Amphidinium carterae</i> Hulburt	K-0654	AY455669
<i>Amphidinium herdmanii</i> Kofoid & Swezy	K-0655	AY455675
<i>Amphidinium massartii</i> Biecheler	CCMP1821	AY455670
<i>Amphidinium gibbosum</i> (Maranda & Shimizu) Flø Jørgensen & Murray	CCMP120	AY455672
<i>Ceratium fusus</i> (Ehrenberg) Dujardin	–	AF260390
<i>Ceratium lineatum</i> (Ehrenberg) Cleve	–	AF260391
<i>Ceratium tripos</i> (O.F. Müller) Nitzsch	–	AF260389
<i>Dinophysis norvegica</i> Claparaède & Lachmann	– (single cell)	AY571375
<i>Gonyaulax baltica</i> Ellegaard, Lewis & Harding	K-0487	AF260388
<i>Gonyaulax baltica</i>	UW394	AY154962
<i>Gonyaulax digitalis</i> (Pouchet) Kofoid	UW415	AY154963
<i>Gonyaulax elongata</i> (Reid) Ellegaard, Daugbjerg, Rochon, J. Lewis & I. Harding	UW388	AY154964
<i>Gymnodinium catenatum</i> L.W. Graham	–	AF200672
<i>Gymnodinium chlorophorum</i> Elbrächter & Schnepf	K-0539	AF200669
<i>Gymnodinium fuscum</i> (Ehrenberg) Stein	CCMP1677	AF200676
<i>Gymnodinium impudicum</i> (Fraga & Bravo) Gert Hansen & Moestrup	JL30	AF200674
<i>Gymnodinium nolleri</i> Ellegaard & Moestrup	K-0602	AF200673
<i>Gyrodinium dominans</i> Hulburt	–	AY571370
<i>Gyrodinium rubrum</i> (Kofoid & Swezy) Takano & Horiguchi	– (single cell)	AY571369
<i>Gyrodinium spirale</i> (Bergh) Kofoid & Swezy	– (single cell)	AY571371
<i>Heterocapsa arctica</i> Horiguchi	CCMP 445	AY571372
<i>Heterocapsa rotundata</i> (Lohmann) Gert Hansen	K-0479	AF260400
<i>Heterocapsa triquetra</i> (Ehrenberg) F. Stein	K-0447	AF260401
<i>Karenia brevis</i> (Davis) Gert Hansen & Moestrup	JL32	AF200677
<i>Karenia mikimotoi</i> (Miyake & Kominami ex Oda) Gert Hansen & Moestrup (DK)	K-0579	AF200682
<i>Karenia mikimotoi</i> (J)	–	AF200681
<i>Karlodinium micrum</i> (Leadbeater & Dodge) J. Larsen	K-0522	AF200675
<i>Peridiniella catenata</i> (Levander) Balech	K-0543	AF260398
<i>Peridinium bipes</i> F. Stein	AJC8-847	AF260385
<i>Peridinium cinctum</i> (O.F. Müller) Ehrenberg	AJC4cl-a	AF260394
<i>Peridinium willei</i> Huitfeldt-Kaas	AJC2-675	AF260384
<i>Polarella glacialis</i> Montresor, Procaccini & Stoecker	–	AY571373
<i>Prorocentrum micans</i> Ehrenberg	K-0335	AF260377
<i>Prorocentrum minimum</i> (Pavillard) Schiller	K-0010	AF260379
<i>Prorocentrum rhathymum</i> Loeblich, Sherley & Schmidt	JL-35	AF260378
<i>Protoceratium reticulatum</i> Bütschli	K-0485	AF260386
<i>Scrippsiella trochoidea</i> var. <i>aciculifera</i> Montresor	K-0500	AF260393
<i>Togula britannica</i> (Herdman) Flø Jørgensen, Murray & Daugbjerg	K-0658	AY455679
<i>Togula compacta</i> (Herdman) Flø Jørgensen, Murray & Daugbjerg	K-0659MFJ16	–
<i>Togula jolla</i> Flø Jørgensen, Murray & Daugbjerg	LB1562	AY455680
<i>Woloszynskia tenuissima</i> (Lauterborn) Thompson	SCCAP K-0666	AY571374
CILIOPHORA		
<i>Euplotes aediculatus</i> Pierson	–	AF223571
<i>Spathidium amphoriforme</i> Greeff	–	AF223570
<i>Tetrahymena thermophila</i> Nanney & McCoy	B1868VII	X54512
<i>Tetrahymena pyriformis</i> (Ehrenberg) Lwoff	GL-C	X54004
Apicomplexa		
<i>Plasmodium falciparum</i> Welch	CAMP	U21939
<i>Toxoplasma gondii</i> Nicolle & Manceaux	RH	X75429

pressum seems to be quite different compared to *Gyrodinium spirale*, as the 'capsule' is located outside and at some distance from the nuclear envelope. In addition, the nuclear pores are not situated in specialised invaginations of the nuclear envelope, although, in *Cochlodinium* (spp.?), chamber-like elevations of the inner fibrillar layer with pores may correspond to the globular chambers of *G. spirale*. However, as in *Erythroopsis* (spp.?), the skeletal layer is clearly separated from the nuclear envelope by vesicles and ribosomes. Hollande et al. (1962) provided some ultrastructural observations on *Plectodinium nucleovolvatum* Biecheler. This species is interesting, as it is morphologically very similar to *G. spirale*, but differs by the presence of an apical spicule and a well-developed nuclear capsule. The latter consists of a hexagonal mesh with minute poroids or caniculi circumscribing larger circles or pores that are visible under the light microscope (Biecheler 1934; Taylor 1987). Although the fixation by Hollande is not optimal, it reveals the presence of a very thick wall-like layer penetrated by numerous pores measuring about 300 nm in diameter. These pores correspond to the small caniculi observed by light microscopy by Biecheler (1934). Subtending the thick layer is a second layer that appears to form 'invaginations' at regular intervals. These somewhat collapsed invaginations are aligned with the pores of the thick layer. Surface sections reveal the inner layer to form a coherent mesh marking the boundary of the large circles visible under the light microscope. It is not clear whether these wall-like layers are situated within or underneath the nuclear envelope. However, the arrangement of the nuclear capsule in *Plectodinium nucleovolvatum* might be quite similar to that of *G. spirale*.

Details of the nuclear capsule have also been provided for *Polykrikos kofoidii* Chatton and *Actiniscus pentasterias* (Ehrenberg) Ehrenberg (Bradbury et al. 1983; Hansen 1993). The capsules of these species are essentially alike and consist of a fibrous layer measuring about 75–100 nm in thickness and located beneath the nuclear envelope. In *P. kofoidii*, this layer consists of two distinct 'sub-layers' of different electron density measuring 34 nm and 79 nm, respectively (Bradbury et al. 1983); whereas in *Actiniscus pentasterias*, one of the sub-layers is very thin or absent. In both species, the layer is penetrated by numerous openings about 100–200 nm in diameter, and more or less globular invaginations (evaginations in *P. kofoidii*) of the nuclear envelope occur in these areas. The nuclear pores are restricted to these invaginations.

It is apparent that some dinoflagellates, notably the unarmoured gymnodinioids, display a remark-

able variation and evolutionary 'experimentation' with respect to reinforcement of the nucleus. Still, it seems obvious that the 'capsule' in *Gyrodinium spirale* and *Plectodinium nucleovolvatum* are quite similar in their basic construction. The inner layer of *Cochlodinium* (spp.?) also shows some resemblance to the capsule of *Gyrodinium spirale*. However, the thick skeletal layer appears to be located outside the nuclear envelope. Although the capsule of *Polykrikos kofoidii* and *Actiniscus pentasterias* is situated underneath the nuclear envelope, it has some elements that resemble *Gyrodinium spirale*. Thus, the invaginations of the nuclear envelope may be homologous with the globular chambers of *G. spirale*, and also the nuclear chambers of *Gymnodinium sensu Daugbjerg et al.* (2000).

The flagellar apparatus: The flagellar apparatus basically resembles that of other dinoflagellates. The most conspicuous difference is the exceptionally long striated root connective between the TSR with the LMR and the bifurcating TSR. Except for *Gymnodinium fuscum* and the zoospore of *Noctiluca scintillans* that lack a TSR (Hansen et al. 2000b; Höhfeld and Melkonian 1995), most dinoflagellates possess an LMR, a TSR, and a src connecting the LMR and the TSR. A src was not observed in *Peridiniella catenata*, but dense material surrounding the LB seemed to mediate the linkage between the LMR and TSR (Hansen and Moestrup 1998). *Peridinium cinctum* and *Peridiniopsis borgei* Lemmermann also lack a src, but instead possess a layered structure (LC) that connects the TSR to electron-opaque material on the dorsal side of the LMR (Calado et al. 1999; Calado and Moestrup 2002). The LC has been suggested to be a characteristic of peridinioid dinoflagellates as it is also present in *Peridiniopsis berlinensis* (Lemmermann) Bourrelly, *Peridinium foliaceum* (Levander) Lemmermann and perhaps in *Heterocapsa pygmaea* Loeblich, Schmidt & Sherley (see Calado et al. 1999). Although a src is also absent in the primitive dinoflagellate *Oxyrrhis marina* Dujardin, it shows a very distinctive root (the LSR) with exactly the same banding pattern as the src of *G. spirale* running from the proximal part of the LB and along the TSR (Roberts 1985). A small, striated connective appears to connect this root with electron dense material located around the LB and the dorsal side of the LMR (Roberts 1985, see Figs 13–14). Although the function of these roots is unknown, the examples show that some sort of linkage between the LMR and TSR is necessary for their proper function.

A dorsal fibrous component of the LMR similar to that observed in *G. spirale* has also been found in the unarmoured *Actiniscus pentasterias* and *Gymno-*

Table 2. Distribution of selected morphological characters in the type species of *Gyrodinium* and *Gymnodinium* (+ = present; – = absent).

Characters	<i>Gyrodinium spirale</i>	<i>Gymnodinium fuscum</i> *
Apical groove	elliptical bisected	horseshoe-shaped
Chloroplasts	–	+
Cortical microtubules	bundles or rows	triangular bundles
Trichocysts	+	–
Nuclear envelope	complex ‘nuclear capsule’	nuclear chambers
Peduncle	–	–
Pusule	tubular collecting chamber	internal vesicular collecting chamber
Pyrenoid	–	–
Striated collars	–	–
Surface ridges	+	–
Ventral ridge	+	–
Flagellar apparatus		
Dorsal fibrous material	+	–
LMR (R1)	+	+
nfc	–	+
src	+	+
TMR (R3)	+	+
TMRE	+	+
TSR	+	–
TSRM (R4)	+	–
Ventral connective (vc)	–	+

*Compiled from Hansen et al. (2000b).

dinium aureolum (Hulburt) Gert Hansen (Hansen 1993, 2001) and it also seems to be present in *G. nolleri* (Ellegaard and Moestrup 1999, their Figs 12, 31–34). However, a fibrous component or connective is also present on the dorsal side of the LMR in the gonyaulacoid *Ceratium furcoides* (Levander) Langhans, a heavily armoured dinoflagellate (Roberts 1989 as *C. hirundinella* (O.F. Müller) Dujardin). It is possible that the electron-opaque material on the dorsal side of the LMR of *Peridinium cinctum* and *Peridiniopsis borgei* (see above) represent this fibrous material.

Of particular interest is a comparison of the FA in *Gyrodinium spirale* and *Gymnodinium fuscum* (the type species of these respective genera) as well as with other species of the *Gymnodinium* group *sensu* Daugbjerg et al. (2000) (Table 2). The most significant difference is the absence in *Gyrodinium spirale* of a nuclear fibrous connective (NFC) linking the FA with the nucleus. This was one of the characters used by Daugbjerg et al. (2000) to redefine the genus *Gymnodinium*. However, it should be noted that both *Actiniscus pentasterias* and *Polykrikos kofoidii* have a NFC, and although they most likely are

closely related to the *Gymnodinium* group, they are not presently considered to be members of the group.

The absence of a ventral connector (vc) in *G. spirale*, but its presence in *G. fuscum*, *G. aureolum*, and *G. nolleri* is noteworthy. This fibre, which connects the ventral side of the LMR with the sulcus, is also present in *Actiniscus pentasterias* and *Akashiwo sanguinea* (Hansen 1993; Roberts and Roberts 1991) and is possibly a characteristic feature of gymnodinoid dinoflagellates at a higher taxonomic level.

The ventral ridge: ventral ridge has been observed in numerous dinoflagellates. It was first observed in *Amphidinium carterae* and referred to as a ‘thickened ridge’ (Dodge and Crawford 1968), then in *Oxyrrhis marina* and termed the ‘ventral ridge’ (Dodge and Crawford 1971). It usually spans the distance between the exit pores of the flagella, but it may also continue to the opening of a feeding tube or peduncle (e.g. Calado et al. 1998). Microtubules are often located parallel to the ridge (e.g. Farmer and Roberts 1989; Höhfeld and Melkonian 1995). The ventral ridge of *G. spirale* is very long and dis-

tinct, but otherwise does not differ from others species. The function of the ridge is uncertain, but centrion is present in the ventral ridge of *Oxyrrhis marina*, suggesting that it may be contractile (Höhfeld et al. 1994). In this species, the ventral ridge (vr) and the ventral ridge microtubules (vrn) terminate at the inner upper part of a non-permanent cytostome. It is made by 'lifting' of the anterior cortical microtubules towards the vrn, and it has been suggested that the vrn and vr play an indirect role in the formation of the cytostome by preventing dislocation of the cortical microtubules (Höhfeld and Melkonian 1998). Food uptake in *Gyrodinium spirale*, like in *O. marina*, is by direct engulfment of prey organisms (e.g. Hansen 1992), and although ultrastructural details of the food uptake are unknown a similar mechanism of the vrn and vr may be present in *G. spirale*. Brown et al. (1988) reported a peduncle in their material of *G. spirale*, but the true identity of this structure is dubious as it contained both mitochondria and trichocysts, which do not normally occur in a peduncle. We have not observed a peduncle-like structure in our material.

Comparison of selected characters: Selected characters of the type species of *Gyrodinium* (*G. spirale*) and *Gymnodinium* (*G. fuscum*) are shown in Table 2. It is apparent that numerous characters, e.g. details of the nuclear capsule, apical groove, arrangement of the cortical microtubules, presence of surface ridges and the absence of a TSR, separate the two type species. The very complex nuclear capsule and the substructure of the surface ridges of *G. spirale* may be synapomorphic characters of the genus *Gyrodinium*.

Phylogeny and evolution of *Gyrodinium*: In this study, we have shown that *Gyrodinium*, with three species including the type, forms a separate evolutionary lineage supported by high bootstrap values ($\geq 92\%$). However, the deep branch lengths separating most of the remaining lineages of dinoflagellates included were characterized by being very short. This indicates that either these lineages of dinoflagellates diverged at the same evolutionary time span or that the LSU rDNA gene is not useful to suggest sister group relationships. A recent phylogenetic analysis by Takano and Horiguchi (2004), using SSU rDNA, also revealed heterotrophic species with surface ridges and an elliptical apical groove as a distinct clade. Within this clade, *Gyrodinium spirale* and *G. fusiforme* clustered together in one group whereas *G. helveticum* (Penard) Takano & Horiguchi (syn: *Gymnodinium helveticum* Penard) and *G. rubrum* (syn: *Gymnodinium rubrum* Kofoid & Swezy) formed another group. At present, the morphological and ultrastructural basis for these relationships are un-

certain. Interestingly, *G. dominans*, *G. helveticum*, and *G. rubrum* all possess a nuclear capsule (Hansen and Larsen 1992; Kofoid and Swezy 1921; pers. obs.), but whether they have the same structure as in *G. spirale* is not known. *Gyrodinium rubrum* has a very thick and characteristic capsule when seen under the light microscope (Hansen and Larsen 1992). Details of the capsule may thus be useful for establishing the phylogeny of *Gyrodinium* species.

DNA sequences from dinoflagellates not yet in culture: The difficulty involved in establishing and maintaining clonal cultures of heterotrophic dinoflagellates (e.g. *Diplopsalis*, *Gyrodinium*, *Polykrikos*, *Protoperidinium*, and *Warnowia*) has resulted in a bias towards autotrophic species in many recent attempts to elucidate the phylogeny and evolutionary history of dinoflagellates using molecular markers (e.g. Daugbjerg et al. 2000; Saldarriaga et al. 2001; Saunders et al. 1997). This is unfortunate since approximately half of all known free-living dinoflagellates are exclusively heterotrophic (Gaines and Elbrächter 1987). Thus, the phylogeny of a substantial part of the dinoflagellates still remains elusive. To overcome this problem, we designed a reverse PCR primer specific to dinoflagellates among all protists presently available in GenBank, which in combination with D1F amplifies ca. 1800 base-pairs of the LSU rDNA gene from dinoflagellates present in marine and freshwater ecosystems (see Methods for primer sequence of 'DINO-ND'). This allowed us to avoid using the eukaryotic primers D1F and D2C applied in similar studies. The *Rhodomonas* culture used as prey for growing *Gyrodinium dominans* was consequently not an obstacle for obtaining the dinoflagellate LSU rDNA sequence when DNA from both organisms was co-extracted from the same culture prior to PCR amplification. The primer 'DINO-ND' also reduces the likelihood of false positives when performing single-cell PCR. However, it has one drawback. If dinoflagellates isolated from freshly collected samples have fed on other dinoflagellates, it is likely that a double sequence will appear in the chromatograms. We did not experience this in any of the dinoflagellate sequences originating from live or fixed samples, although *G. spirale* is known to engulf other dinoflagellates (see Fig. 21). One possible solution for handling double sequences would be to clone the PCR products. A general drawback of using single-cell PCR analysis is obviously that no DNA is stored for completing the partial LSU rDNA gene sequence or for determination of additional gene sequences.

Contrary to what was concluded in a recent study by Godhe et al. (2002), we managed to amplify ap-

prox. 1800 base-pairs of the LSU rDNA gene from a single cell of *G. spirale* micro-pipetted from a water sample fixed in 5% Lugol's solution and kept in the dark for 6 months at a low temperature. Other researchers have also successfully amplified DNA sequences from organisms fixed in Lugol's solution (e.g. Bowers et al. 2000; Guillou et al. 2002). Amplifying DNA by using group-specific primers has great potential with live or fixed cells provided that identification is possible. The approach we have applied here combining a group-specific primer on isolated single cells represents a good candidate for future inclusions of the many species of heterotrophic dinoflagellates in phylogenetic studies.

Methods

Light and scanning electron microscopy: Material for light microscopical and SEM observations was obtained from a water sample collected in Skagerrak, near Hirtshals, Denmark, in May 2000. For SEM, single cells were isolated and placed onto Nuclepore filters (8 µm pore size) mounted in a Swinnex filterholder (Millipore) filled with sterile filtered seawater. Fixation was in 1% OsO₄ in filtered seawater. The material was fixed for ca. 30 min. The cells were subsequently dehydrated in an ethanol series, critical point dried and sputter coated with gold. The SEM microscope used was a Phillips 515 operated at 25 kV. The light microscope used was an Olympus Provis AX70 with an Olympus PM-20 micro-photosystem.

Electron microscopy: The material for transmission electron microscopy was obtained from a water sample collected in Ballen Harbour, Samsø, Denmark, May 1996. It contained a mixed phytoplankton assemblage dominated by various centric diatoms and heterotrophic dinoflagellates, primarily species of *Protoperdinium*, and a fairly high number of *Gyrodinium spirale* cells.

Two fixation schedules were applied:

Schedule 1. Initial fixation (30 min, 4 °C) was made by adding one volume fixative containing 4% glutaraldehyde made up in 0.1 M Na-cacodylate buffer in filtered seawater to one volume water sample. The material was pelleted and subsequently washed in two changes of buffered seawater, 5 min in each change. The second fixation was in 1% OsO₄ in buffered seawater for 1 h. After a brief rinse in buffered seawater the material was dehydrated in a graded alcohol series and flat-embedded in Spurr's resin via propylene oxide (Hansen 1989). Individual cells of *Gyrodinium spirale* were cut out with a razor blade using a stereomicroscope and remounted on

resin stubs. Serial sections were cut on a Reichert Ultracut E microtome using a diamond knife and collected on slot grids. Sections were double stained in uranyl acetate (made up in 50% methanol) and stained in lead citrate. The electron microscope used was a JEOL-100CX operated at 80 kV.

Schedule 2. Initial fixation (15 min, 4 °C) was made by adding one volume of the fixative containing 4% glutaraldehyde and 0.4 % OsO₄, made in 0.1 M Na-cacodylate buffered filtered seawater, to one volume water sample. The material was pelleted and subsequently washed in two changes of buffered seawater, 5 min in each change. The following steps were identical to those of schedule 1.

Fixation 1 generally gave a better preservation of the internal structure of the cell notably the flagellar apparatus and the nucleus, whereas fixation 2 provided a better preservation of the amphiesma.

Single-cell PCR amplification of *Gyrodinium spirale*, *Gyrodinium rubrum*, and *Dinophysis norvegica*: The prey organisms of many heterotrophic dinoflagellates are unknown and this explains the difficulty in maintaining dinoflagellate cultures over longer time periods, including *G. spirale* and *G. rubrum*. Other dinoflagellates like *Dinophysis* spp. have so far proved virtually impossible to maintain in culture (Maestrini et al. 1995). An alternative way of obtaining DNA from these organisms is to perform PCR on single cells (e.g. Edvardsen et al. 2003; Guillou et al. 2002; Sebastián and O'Ryan 2001). Here, it was performed by micropipetting individual cells (i.e. *G. spirale*, Fig. 54) from water samples from the North Sea, collected in August 2002 and fixed in acidified Lugol's solution, or from live material from Kattegat, Denmark, collected in March and September 2000 (i.e. *G. rubrum* and *D. norvegica*) using an inverted microscope. Single cells were rinsed at least four times in distilled seawater (30 PSU) to prevent contamination of foreign DNA and finally placed with as little seawater as possible in a 0.5 mL Eppendorf tube containing 8 µl ddH₂O. Since the PCR primers typically used to amplify LSU rDNA are eukaryote-specific, they will amplify any eukaryote present in the PCR tube. To prevent amplification of non-dinoflagellate LSU rDNA, a reverse primer specific to dinoflagellates (see Discussion) was designed and labelled 'Dino-ND': 5'-ACACCTCGGAAGACAAGGT-3'. This primer in combination with D1R-F (Scholin et al. 1994) was used to amplify approx. 1800 base-pairs from single cells of *G. spirale*, *G. rubrum*, and *Dinophysis norvegica*. These two external primers in addition to the internal primers already listed in Daugbjerg et al. (2000) were used for sequence determination. To verify the LSU rDNA sequence determined by single-cell PCR analysis of *G. rubrum*, the procedure

was repeated using another single cell of *G. rubrum*. The sequences obtained were identical and the technique reproducible. PCR conditions, purification of PCR products, and nucleotide sequencing were as previously described (Hansen et al. 2003).

DNA extraction of *Gyrodinium dominans*: *Gyrodinium dominans* is heterotrophic and may be kept for longer time in culture by using the cryptophyte *Rhodomonas salina* (Wislouch) Hill & Wetherbee as food source. The material used in this study originated from a water sample from Øresund, Denmark collected in the fall 1997. The procedure used to extract total genomic DNA and determine partial LSU rDNA was outlined in Hansen et al. (2003), except that we used the dinoflagellate-specific reverse primer to avoid amplification of DNA from the cryptophyte.

DNA extraction of clonal cultures of *Heterocapsa arctica*, *Polarella glacialis*, and *Woloszynskia tenuissima*: During this study we also determined partial LSU rDNA sequences from three additional dinoflagellates in culture. *Heterocapsa arctica* (CCMP 445) was obtained from the Provasoli-Guilford National Center for Marine Phytoplankton. *Polarella glacialis* was isolated into clonal culture by micropipetting a cell from a water sample collected in the Ross Sea, Antarctica (during an expedition onboard M/S N.B. Palmer December 1998–February 1999). A clonal culture of *Woloszynskia tenuissima* was also isolated by micropipetting a single cell from a water sample collected at Lake Helen, Kangerlussuaq, Greenland. DNA extraction and sequencing is outlined in Hansen et al. (2003).

Alignment and phylogenetic analyses of LSU rDNA: The new sequences of *Gyrodinium spirale*, *G. dominans*, *G. rubrum*, *Dinophysis norvegica*, *Polarella glacialis*, *Woloszynskia tenuissima*, and *Heterocapsa arctica* were aligned with 39 dinoflagellate LSU rDNA sequences available in GenBank. Four ciliates and two apicomplexa were included for outgroup-rooting (Table 1) as molecular studies have shown them to form sister groups to the dinoflagellates (e.g. Van de Peer et al. 1996). The data matrix comprising the 45 sequences were aligned by incorporating information from the secondary structure of LSU rRNA as suggested by De Rijk et al. (2000). The alignment comprised 1655 base-pairs, including introduced gaps, corresponding to 44 base-pairs upstream domain D1 to 20 base-pairs downstream domain D6 (see Lenaers et al. 1989). Among these, we excluded a fragment consisting of 350 base-pairs because it could not be confidently aligned. This fragment started at nucleotide 10 within the highly variable domain D2 and stopped 12 nucleotide before the end of domain D2 (see Lenaers et al. 1989). The alignment can be downloaded at

<http://www.bi.ku.dk/staff/nielsd/protist2004.htm>. The remaining 1305 base pairs were analysed using Maximum Likelihood (ML), Maximum Parsimony (MP), and Neighbor-joining (NJ) methods using PAUP* version 4.0b10 (Swofford 2003). Prior to ML analyses, we used Modeltest (version 3.06 by Posada and Crandall 1998) to find the best model for the LSU rDNA sequences using hierarchical likelihood ratio tests. The best-fit model was TrN+I+G (Tamura and Nei 1993) with among-sites rate heterogeneity ($\alpha = 0.6600$), an estimated proportion of invariable sites ($I = 0.1536$), and two substitution rate categories (A–G = 2.6274 and C–T = 5.28). Base frequencies were set as follows A = 0.2846, C = 0.1722, G = 0.2462 and T = 0.297. Due to computational constraints, only 100 replicates were performed in ML bootstrap analyses using the ‘fast step-wise’ addition option. In MP analysis, 1000 random additions were performed using the heuristic search option and a branch-swapping algorithm (tree-bisection-reconnection). All characters were unordered, equally weighted and gaps were treated as missing data. For parsimony bootstrap analyses, 1000 replicates were performed.

The same model as in ML analysis was applied to compute dissimilarity values. This distance matrix was used to build a tree with the Neighbor-joining (NJ) method. Bootstrap values for the NJ tree were based on 1000 replicates.

Acknowledgements

We thank Øjvind Moestrup and Antonio Calado for critically reading of the manuscript. Hans H. Jacobsen is thanked for providing the culture of *Gyrodinium dominans* and Charlotte Hansen for running our sequences on the ABI 377. Yoshihito Takano and Takeo Horiguchi are appreciated for access to unpublished results. ND thanks the Carlsberg Foundation for equipment grants (970410/40-1238 and 990906/40-1215). This study was supported by the Danish Science Research Council (project #21-02-0539) to ND and the Carlsberg Foundation to GH.

References

- Bergh RS** (1881) Organismus der Cilioflagellaten. Eine phylogentische Studie. Wilhelm Engelmann, Leipzig, 288 pp
- Biecheler B** (1934) Sur une Dinoflagellé a capsule périnucléaire, *Plectodinium*, n. gen. *nucleovolvatum*, n. sp. et sur les relations des Péridiniens avec les Radiolaires. CR Hebd Séanc Acad Sci Paris **198**: 404–406

- Bowers HA, Tengs T, Glasgow HB, Burkholder JM, Rublee PA, Oldach DW** (2000) Development of real-time PCR assays for rapid detection of *Pfiesteria piscicida* and related dinoflagellates. *Appl Environ Microbiol* 66: 4641–4648
- Bradbury PC, Westfall JA, Townshend JW** (1983) Ultrastructure of the dinoflagellate *Polykrikos*. II. The nucleus and its connection to the flagellar apparatus. *J Ultrastruct Res* **85**: 24–32
- Brown DL, Cachon J, Cachon M, Boillot A** (1988) The cytoskeletal microtubular system of some naked dinoflagellates *Cell Motil Cytoskeleton* **9**: 361–374
- Calado AJ, Moestrup Ø** (2002) Ultrastructural study of the type species of *Peridiniopsis*, *Peridiniopsis borgei* (Dinophyceae), with special reference to peduncle and flagellar apparatus. *Phycologia* **41**: 567–584
- Calado AJ, Craveiro SC, Moestrup Ø** (1998) Taxonomy and ultrastructure of a freshwater heterotrophic *Amphidinium* (Dinophyceae) that feeds on unicellular protists. *J Phycol* **34**: 536–554
- Calado AJ, Hansen G, Moestrup Ø** (1999) Architecture of the flagellar apparatus and related structures in the type species of *Peridinium*, *P. cinctum* (Dinophyceae). *Eur J Phycol* **34**: 179–191
- Daugbjerg N, Hansen G, Larsen J, Moestrup Ø** (2000) Phylogeny of some of the major genera of dinoflagellates based on ultrastructure and partial LSU rDNA sequence data, including the erection of three new genera of unarmoured dinoflagellates. *Phycologia* **39**: 302–317
- De Rijk P, Wuyts J, van der Peer Y, Winkelmanns T, de Wachter R** (2000) The European large subunit ribosomal RNA database. *Nucleic Acids Res* **28**: 117–118
- Dodge JD** (1972) The ultrastructure of the dinoflagellate pusule: A unique osmo-regulatory organelle. *Protoplasma* 75: 285–302
- Dodge JD** (1982) Marine Dinoflagellates of the British Isles. Her Majesty's Stationery Office, London, 303 pp
- Dodge JD, Crawford RM** (1968) Fine structure of the Dinoflagellate *Amphidinium carteri* Hulbert [sic.]. *Protistologica* **4**: 231–248
- Dodge JD, Crawford RM** (1970) A survey of the thecal fine structure in the Dinophyceae. *Bot J Linn Soc* **63**: 53–67
- Dodge JD, Crawford RM** (1971) Fine structure of the dinoflagellate *Oxyrrhis marina*. Part 2: the flagellar system. *Protistologica* **7**: 399–409
- Edvardsen B, Shalchian-Tabrizi K, Jakobsen KS, Medlin LK, Dahl E, Brubak S, Paasche E** (2003) Genetic variability and molecular phylogeny of *Dinophysis* species (Dinophyceae) from Norwegian waters inferred from single cell analysis of rDNA. *J Phycol* **39**: 395–408
- Ellegaard M, Moestrup Ø** (1999) Fine structure of the flagellar apparatus and morphological details of *Gymnodinium nolleri* sp. nov. (Dinophyceae), an unarmoured dinoflagellate producing a microreticulate cyst. *Phycologia* **38**: 289–300
- Ellegaard M, Daugbjerg N, Rochon A, Lewis J, Harding I** (2003) Morphological and LSU rDNA sequence variation within the *Gonyaulax spinifera*/*Spiniferites*-group (Dinophyceae) and proposal of two new combinations, *Gonyaulax elongata* comb. nov. and *G. membranacea* comb. nov. *Phycologia* **42**: 151–164
- Farmer MA, Roberts KR** (1989) Comparative analysis of the dinoflagellate flagellar apparatus. III. Freeze substitution of *Amphidinium rhyncocephalum*. *J Phycol* **25**: 280–292
- Fensome RA, Taylor FJR, Norris G, Sarjeant WAS, Wharton DI, Williams GL** (1993) A classification of living and fossil dinoflagellates. *Micropaleontology Spec Publ No. 7*. Am Mus Nat Hist, Hanover, PA, 351 pp
- Flø Jørgensen M, Murray S, Daugbjerg N** (2004) *Amphidinium* revisited: I. Redefinition of *Amphidinium* (Dinophyceae) based on cladistic and molecular phylogenetic analyses. *J Phycol* **40**: 351–365
- Gaines G, Elbrächter M** (1987). Heterotrophic Nutrition. In Taylor FJR (ed) *The Biology of Dinoflagellates*. Blackwell Scientific Publications, Oxford, pp 224–268
- Godhe A, Rehnstam-Holm A-S, Karunasagar I, Karunasagar I** (2002) PCR detection of dinoflagellate cysts in field sediment samples from tropic and temperate environments. *Harmful Algae* 1: 361–373
- Greuet C** (1972) Intervention de lamelles annelées dans la formation de couches squelettiques au niveau de la capsule périnucléaire de péridiniens Warnowiidae. *Protistologica* **8**: 155–168
- Greuter W, Burdet HM, Chaloner WG, Demoulin, V, Grolle DL, Hawksworth DL, Nicholson DH, Silva PC, Stafleu FA, Voss EG, McNeill J** (1988) International code of botanical nomenclature. *Regnum Veg* **118**: 126
- Guillou L, Nézan E, Cueff V, Erard-Le Denn E, Cambon-Bonavita M-A, Gentien P, Barbier G** (2002). Genetic diversity and molecular detection of three toxic dinoflagellate genera (*Alexandrium*, *Dinophysis*, and *Karenia*) from French coasts. *Protist* 153: 223–238
- Hansen G** (1989) Ultrastructure and morphogenesis of scales in *Katodinium rotundatum* (Lohmann) Loeblich (Dinophyceae). *Phycologia*: **28**: 385–394
- Hansen G** (1993) Light and electron microscopical observations of the dinoflagellate *Actiniscus pentasterias* (Dinophyceae). *J Phycol* **29**: 486–499
- Hansen G** (2001) Ultrastructure of *Gymnodinium aureolum* (Dinophyceae): toward a further redefinition of *Gymnodinium* sensu stricto. *J Phycol* 37: 612–623
- Hansen G, Larsen J** (1992) Dinoflagellater i Danske Farvande. In Thomsen HA (ed) *Plankton i indre Danske Farvande*. National Agency of Environmental Protection, Copenhagen pp 45–155

- Hansen G, Moestrup Ø** (1998) Light and electron microscopical observations of *Peridiniella catenata* (Dinophyceae). *Eur J Phycol* **33**: 293–305
- Hansen G, Daugbjerg N, Franco JM** (2003) Morphology, toxin composition and LSU rDNA phylogeny of *Alexandrium minutum* (Dinophyceae) from Denmark, with some morphological observations on other European strains. *Harmful Algae* **2**: 317–335
- Hansen G, Daugbjerg N, Henriksen P** (2000a) Comparative study of *Gymnodinium mikimotoi* and *Gymnodinium aureolum* comb. nov. (= *Gyrodinium aureolum*) based on morphology, pigment composition, and molecular data. *J Phycol* **36**: 394–410
- Hansen G, Moestrup Ø, Roberts KR** (2000b) Light and electron microscopical observations on the type species of *Gymnodinium*, *G. fuscum* (Dinophyceae). *Phycologia* **39**: 365–376
- Hansen PJ** (1992) Prey size selection, feeding rates and growth dynamics of heterotrophic dinoflagellates with special emphasis on *Gyrodinium spirale*. *Mar Biol* **114**: 327–334
- Hollande A, Cachon J, Cachon-Enjumet M** (1962) Mise en évidence par la microscopie électronique, d'une capsule centrale chez divers péridiniens. Considérations sur les affinités entre dinoflagellés et radio-laires. *CR Hebd Séanc Acad Sci Paris* **254**: 2069–2071
- Honsell G, Talarico L, Cabrini M** (1988) Interesting ultrastructural features of a green dinoflagellate. *G Bot Ital* **122**: 76–78
- Höhfeld I, Melkonian M** (1992) Amphiesmal ultrastructure of dinoflagellates: a reevaluation of pellicle formation. *J Phycol* **28**: 82–89
- Höhfeld I, Melkonian M** (1995) Ultrastructure of the flagellar apparatus of *Noctiluca miliaris* Suriray swarmers (Dinophyceae). *Phycologia* **34**: 508–513
- Höhfeld I, Melkonian M** (1998) Lifting the curtain? The microtubular cytoskeleton of *Oxyrrhis marina* (Dinophyceae) and its rearrangement during phagocytosis. *Protist* **149**: 75–88
- Höhfeld I, Beech PL, Melkonian M** (1994) Immunolocalization of centrin in *Oxyrrhis marina* (Dinophyceae). *J Phycol* **30**: 474–489
- Kimball JF, Wood EJF** (1965) A dinoflagellate with characters of *Gymnodinium* and *Gyrodinium*. *J Protozool* **12**: 577–580
- Kofoid CA, Swezy O** (1921) The Free-Living Unarmoured Dinoflagellata. *Memoirs of the University of California* **5**: 1–564
- Larsen J** (1988) An ultrastructural study of *Amphidinium poecilochroum* (Dinophyceae), a phagotrophic dinoflagellate feeding on small species of cryptophytes. *Phycologia* **27**: 366–377
- Leadbeater B, Dodge JD** (1966) The fine structure of *Woloszynskia micra* sp. nov., a new marine dinoflagellate. *Br Phycol Bull* **3**: 1–17
- Lenaers G, Maroteaux L, Michot B, Herzog M** (1989) Dinoflagellates in evolution. A molecular phylogenetic analysis of large subunit ribosomal RNA. *J Mol Evol* **29**: 40–51
- Maestrini SY, Berland RB, Grzebyk D, Spanò AM** (1995) *Dinophysis* spp. cells concentrated from nature for experimental purposes, using size fractionation and reverse migration. *Aquat Microb Ecol* **9**: 177–182
- Melkonian M, Höhfeld I** (1988) Amphiesmal ultrastructure in *Noctiluca miliaris* Suriray (Dinophyceae). *Helgol Meeresunters* **42**: 601–612
- Moestrup Ø** (2000) The Flagellate Cytoskeleton: Introduction of a General Terminology for Microtubular Roots in Protists. In Leadbeater BSC, Green JC (eds) *The flagellates. Unity, Diversity and Evolution*. Syst Assoc Spec Vol 59. Taylor and Francis, London, pp 67–94
- Morill LC, Loeblich AR III** (1983) Formation and release of body scales in the dinoflagellate genus *Heterocapsa*. *J Mar Biol Assoc UK* **63**: 905–913
- Pickett-Heaps JD, Schmid A-MM, Edgar LA** (1990) The Cell Biology of Diatom Valve Formation. In Round RE, Chapman DJ (eds) *Progress in Phycological Research*, Biopress, Bristol, Vol 7, pp 1–168
- Posada D, Crandall KA** (1998) MODELTEST: testing the model of DNA substitution. *Bioinformatics* **14**: 817–818
- Roberts KR** (1985) The flagellar apparatus of *Oxyrrhis marina* (Pyrrophyta). *J Phycol* **21**: 641–655
- Roberts KR** (1989) Comparative analysis of the dinoflagellate flagellar apparatus. II. *Ceratium hirundinella*. *J Phycol* **25**: 270–280
- Roberts KR, Roberts JE** (1991) The flagellar apparatus and cytoskeleton of the dinoflagellates. A comparative overview. *Protoplasma* **164**: 105–122
- Sebastián CR, O'Ryan C** (2001) Single-cell sequencing of dinoflagellate (Dinophyceae) nuclear ribosomal genes. *Mol Ecol Notes* **1**: 329–331
- Saldarriaga JF, Taylor FJR, Keeling PJ, Cavalier-Smith T** (2001) Dinoflagellate nuclear SSU rRNA phylogeny suggests multiple plastid losses and replacements. *J Mol Evol* **53**: 204–213
- Saunders GW, Hill DRA, Sexton JP, Andersen RA** (1997) Small-subunit ribosomal RNA sequences from selected dinoflagellates: testing classical evolutionary hypotheses with molecular systematic methods. *Plant Syst Evol Suppl* **11**: 237–259
- Schütt F** (1895) Die Peridineen der Plankton-Expedition. *Ergebnisse der Plankton-Expedition der Humboldt-Stiftung* **4**: 1–170
- Schütt F** (1896) Gymnodiniaceae, Prorocentraceae, Peridiniaceae, Bacillariaceae. In Engler A, Prantl K (eds) *Die natürlichen Pflanzenfamilien*. Wilhelm Engelmann, Leipzig, 1st edition, Teil 1, Abt b, pp 1–153

Scholin CA, Herzog M, Sogin M, Anderson DM (1994) Identification of group- and strain-specific genetic markers for globally distributed *Alexandrium* (Dinophyceae). II. Sequence analysis of a fragment of the LSU rRNA gene. J Phycol **30**: 999–1011

Stein FR von (1883) Der Organismus der Infusionsthiere nach eigenen Forschungen in systematischer Reihenfolge bearbeitet. III. Abteilung. II. Hälfte. Die Naturgeschichte der arthrodelen Flagellaten. Wilhelm Engelmann, Leipzig, 30 pp, 25 pl.

Swofford DL (2003) PAUP* Phylogenetic analysis using parsimony (*and other methods). Version 4. Sinauer Associates, Sunderland, MA

Takano Y, Horiguchi T (2004) Surface ultrastructure and molecular phylogenetics of four unarmoured heterotrophic dinoflagellates, including the type species of the genus *Gyrodinium*. Phycol Res **52**: 107–116

Tamura K, Nei N (1993) Estimation of the number of nucleotide substitutions in the control region of mitochondrial DNA in humans and chimpanzees. Mol Biol Evol **10**: 512–526

Taylor FJR (1987) Dinoflagellate Morphology. In Taylor FJR (ed) The Biology of Dinoflagellates. Blackwell Scientific Publications, Oxford, pp 224–268

Van de Peer Y, Van der Auwera G, De Wachter R (1996) The evolution of stramenopiles and alveolates as derived by “substitution rate calibration” of small ribosomal subunit RNA. J Mol Evol **42**: 201–210

Wilcox LW, Wedemayer GJ, Graham LE (1982) *Amphidinium cryophilum* sp. nov. (Dinophyceae), a new freshwater dinoflagellate. II. Ultrastructure. J Phycol **18**: 18–30